

TECTONOSTRATIGRAPHIC SIGNIFICANCE OF THE NEOGENE SEDIMENTARY RECORD OF NORTHWESTERN AUSTRAL-MAGALLANES BASIN, ARGENTINEAN PATAGONIA

*Inés Aramendía*¹, *José I. Cuitiño*², *Matías Ghiglione*³, *Pablo José Bouza*¹

¹ Instituto Patagónico para el Estudio de Ecosistemas Continentales, CCT-CONICET-CENPAT, Boulevard Almirante Brown 2915, Puerto Madryn U9120A CD, Chubut, Argentina. aramendia@cenpat-conicet.gob.ar; bouza@cenpat-conicet.gob.ar

² Instituto Patagónico de Geología y Paleontología, CCT-CONICET-CENPAT, Boulevard Almirante Brown 2915, Puerto Madryn U9120ACD, Chubut, Argentina. jcuitino@cenpat-conicet.gob.ar

³ Instituto de Estudios Andinos "Don Pablo Groeber" CONICET, Departamento de Ciencias Geológicas, FCEN, Universidad de Buenos Aires. matias@gl.fcen.uba.ar

ARTICLE INFO

Article history

Received November 12, 2018

Accepted May 15, 2019

Available online May 16, 2019

Invited Editor

Augusto N. Varela

Handling Editor

Sebastian Richiano

Keywords

Sedimentology

Miocene

Tectonics

Southern Andes

Patagonia

ABSTRACT

Despite their geodynamic significance, the stratigraphy and paleoenvironments of the lower-middle Miocene clastic deposits, genetically related to subduction-driven lithospheric processes at the latitude of the Chile Triple Junction are poorly known. These beds, outcropping along the foothills of the Southern Patagonian Andes in the northwestern edge of the Austral-Magallanes Basin, include the marine Centinela Formation transitionally covered by the continental Río Zeballos Group. The aim of this work is to present an integrated stratigraphic section and to discuss its paleoenvironmental evolution, based on facies analysis. We inquired into possible tectonic-drivers during continentalization including a short extensional episode affecting the basal Miocene sequences associated to the initial stages of the Andean uplift. We measured a 980 m-thick succession, subdivided into three sedimentary units (SU I, SU II and SU III). The lower SU I is dominated by shallow marine, bioturbated sandstones and heterolithic deposits. SU II is dominated by interbedded medium- to pebbly-grained cross-stratified sandstones and mudstones, interpreted as fluvial channels and floodplains with incipient paleosols. Following, SU II shows a clear upward increase in the sandstone/mudstone ratio. Topping the sequences, SU III is composed of structureless and cross-bedded conglomerates interbedded with coarse-grained sandstones, interpreted as channel and sheet-flood deposits within an alluvial fan. The whole coarsening upward trend, from shallow marine to fluvial and finally to alluvial fan deposits, suggests that these deposits were influenced by a progressive reduction in accommodation space. The sequence is covered by basalts, truncated by a regional relictic surface composed of terrace conglomerates of the Rodados Patagónicos, reflecting basin abandonment and generation of a bypass surface during the late Miocene-Quaternary. Based on our results, published U-Pb detrital ages, and thermochronological data, we relate the evolution of the Neogene sedimentary systems to a synchronous contraction-related eastward migration of the deformation front of the adjacent Andean orogenic belt, followed by neutral tectonics.

INTRODUCTION

The late Cenozoic Andean sedimentary units in the northern Austral-Magallanes Basin preserve evidence of the early Miocene Patagonian marine transgression and the subsequent regression of the Río Zeballos Group and the equivalent Santa Cruz Formation (Giacosa and Franchi, 2001; Escosteguy *et al.*, 2003; Cuitiño *et al.*, 2019). These sequences are located in a retroarc tectonic environment characterized by a complex evolution due to changing subduction rates caused by the interaction between South America and Farallón-Nazca-Antarctic plates, including the collision of the active Chile Spreading Ridge (CSR) in the junction between those plates (Lagabrielle *et al.*, 2004, 2007; Scalabrino *et al.*, 2009; Salze *et al.*, 2018). It is noteworthy the discontinuation of sedimentary deposits close to ~14 Ma (Lagabrielle *et al.*, 2004; Blisniuk *et al.*, 2005; Scalabrino *et al.*, 2009), produced by the dynamic uplift of Patagonia (Guillaume *et al.*, 2013; Dávila *et al.*, 2018) and the instauration of neutral tectonics in the area since the late Miocene (Ghiglione *et al.*, in press).

We analyzed the retroarc sedimentary deposits of the Southern Patagonian Andes (~46° 30' SL), where the northwestern border of the Austral-Magallanes Basin is located (Fig. 1). The general stratigraphic succession in the area starts with a Late Jurassic syn-rift volcanic sequence of the El Quemado Complex, followed by Lower Cretaceous thermal sag deposits represented by the Springhill (Berriasian-Valanginian) and Río Mayer (Hauterivian-Barremian) formations (Aguirre Urreta, 1985; Aguirre Urreta and Ramos, 1981; Richiano *et al.*, 2012, 2015, 2016), covered by the Aptian-Cenomanian post-rift volcanoclastic Río Tarde Formation. After a long hiatus, upper Paleocene-lower Eocene continental quartz-rich deposits of the Ligorio Márquez Formation deposited over the Mesozoic units (Escosteguy *et al.*, 2001, 2003; Encinas *et al.*, 2018a). The Eocene in this area is characterized by volcanic events including intrusions (Jainemeni Teschenite) and basaltic effusions of the Posadas Basalt and immediately followed by the Oligocene effusion of the Sandín Basalt (Escosteguy *et al.*, 2003). The studied lower-middle Miocene synorogenic deposits represent the upper part of the sedimentary succession, composed of the marine Centinela/El Chacay Formation and the continental Río Zeballos Group (Hatcher, 1897, 1900; Ugarte,

1956; Chiesa and Camacho, 1995; Dal Molin and Colombo, 2003; Cuitiño *et al.*, 2015). Finally, these deposits are covered by the 12.4–3.3-Ma-old basaltic Meseta Lago Buenos Aires Formation (Ugarte, 1956; Lapido, 1979; Busteros and Lapido, 1983; Guivel *et al.*, 2006), and glacial, alluvial and gravitational Quaternary deposits (Escosteguy *et al.*, 2003).

The stratigraphic section analyzed in this work records accumulation in a retroarc foreland basin. Foreland basins are elongated regions developed on continental crust near or associated with mountain ranges (DeCelles and Giles, 1996; DeCelles and Cavazza, 1999). Their development is in response to geodynamic processes related to subduction with four clear depozones (DeCelles and Giles, 1996; Horton and DeCelles, 1997): *i) wedge-top* -sediment mass that accumulates on top of the frontal part of the orogenic belt; *ii) foredeep* -sediments deposited between the structural front of the fold and thrust belt and the proximal flank of the forebulge; *iii) forebulge* -broad region of potential flexural uplift between the foredeep and the back-bulge depozones- and *iv) back-bulge* -sediment that accumulates in the shallow but broad zone of potential flexural subsidence cratonward or passive marginward of the forebulge-depозones. The Miocene sedimentary sequences studied in this work are closely related to the onset of Neogene Andean uplift, and record the Middle Miocene abandonment of the foreland basin system of the Austral-Magallanes Basin.

The aim of this paper is to present a detailed sedimentologic field-based facies analysis for the synorogenic Miocene outcrops of the northwestern Austral-Magallanes Basin. Our analysis permits to unravel the sedimentary processes that developed during this particular episode of the basin infill history. We also relate the paleoenvironmental evolution to different tectonic regimes that affected the retroarc of the Southern Patagonian Andes during the Neogene foreland basin regime.

GEOLOGICAL AND STRATIGRAPHIC FRAMEWORK

Geological setting

The analyzed stratigraphic interval is located on the retroarc side of the Southern Patagonian Andes, and constitutes part of the northwestern Miocene deposits of the Austral-Magallanes Basin between 46°30' S and 47°00' S (Fig. 1). This region is

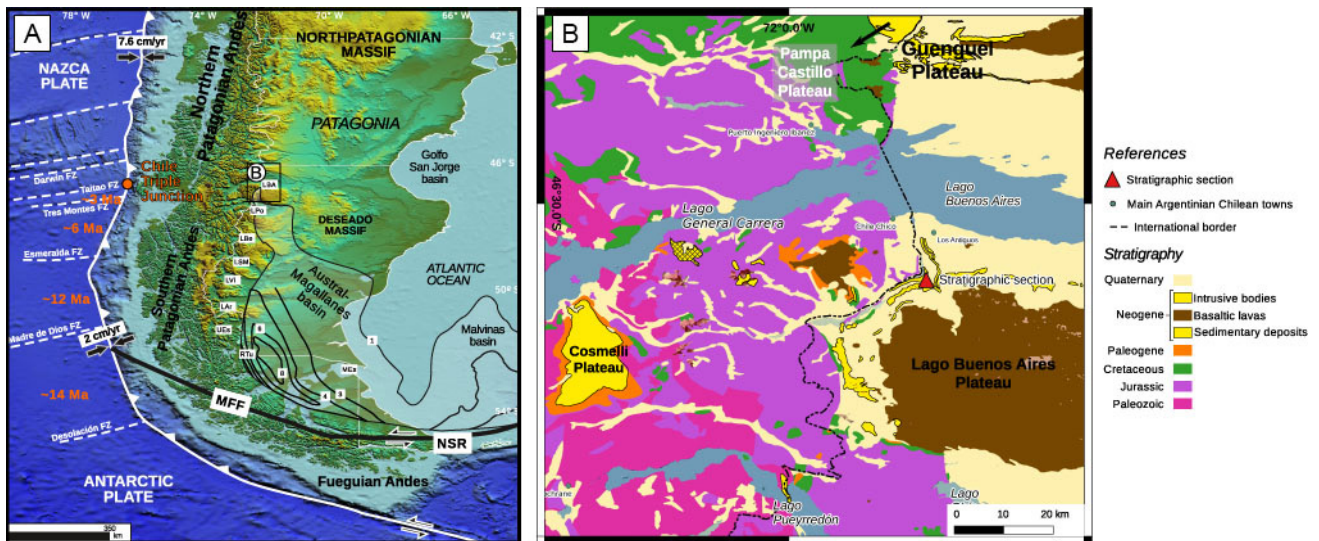


Figure 1. General locations map of the study area and their main morphotectonic blocks. **a)** Location of main morphostructural units and tectonic features mentioned in the text, after Ghiglione *et al.* (2010) and references therein. Orange ages (Ma) in the Pacific trench indicate the time of collision of each ridge segment between oceanic fault zones. MFF Magallanes-Fagnano Fault; LAr Lago Argentino; LBA Lago Buenos Aires; LBe Lago Belgrano; LPo Lago Posadas; LSM Lago San Martín; LVi Lago Viedma; MEs Magallanes Strait; NSR North Scotia Ridge; RTu Río Turbio; UEs Última Esperanza. Contours indicate sediment thickness in kilometers. The black square represents the study area. **b)** Detailed map of the study area showing the location of the main Miocene depocenters, plateaus (igneous and sedimentary genesis) and stratigraphic section.

characterized by several plateaus of different genesis (Fig. 1): sedimentary (*i.e.* Guenguel, Balmaceda and Guadal) and volcanic (*i.e.* Lago Buenos Aires Plateau). In this region, the oldest outcropping rocks are represented by the volcanic El Quemado Complex (Ugarte, 1956; Escosteguy *et al.*, 2003; Lagabrielle *et al.*, 2004, 2007) representing the last episode of the Chon Aike acidic igneous province rifting event (Pankhurst *et al.*, 2000; Sruoga *et al.*, 2014). Overlying in transitional contact a post-rift Cretaceous sequence is developed involving a basin-scale marine transgression (Springhill and Río Mayer formations) and a subsequent volcanic event (Río Tarde Formation). The tectonic setting for the Springhill-Río Mayer formations transgression involves diachronic stages in the retroarc (rift, sag and compressional): in the southern Austral-Magallanes depocenter, the oldest, Late Jurassic (Tithonian), remnants of Springhill Formation are part of the rifting, followed by the Berriasian-Barremian main deposits of the transgression, mostly deposited in a thermal sag to compressional setting (Kraemer, 1998; Varela *et al.*, 2013; Zerfass *et al.*, 2017). In the northern depocenter where our profiles are located, the upper shallow-marine section of the Río Mayer Formation represents the

onset of a Barremian to Aptian highstand systems tract (Richiano *et al.*, 2012; 2015), probably driven by the generalized uplift of surrounding blocks (Aramendía *et al.*, 2018). Aptian-Albian regressive sequences with detrital provenance typical from a compressional setting (Ghiglione *et al.*, 2015), includes the coastal Río Belgrano Formation and the fluvial volcanoclastic deposits of Río Tarde Formation, that prograded from north to south into more regionally distributed marine sequences from Río Mayer Formation (Barberón *et al.*, 2015; 2018).

Unconformably overlaying these deposits, a quartz-rich continental sedimentary unit represented by Ligorio Márquez Formation displays fluvial channels and floodplains deposits interspersed with logs and vegetal remains (Escosteguy *et al.*, 2003). An Eocene effusive volcanic event is represented by the Posadas Basalt and basic intrusive Jeinemeni Teschenite (Suárez *et al.*, 2000; De La Cruz *et al.*, 2003). Superimposed sometimes in sharp contact otherwise covered, the studied Miocene units crop out along the margins of the Jeinemeni and Los Antiguos rivers, close to the Argentina-Chile border. These Neogene synorogenic deposits start with the Patagonian Miocene marine transgression followed by terrestrial deposits.

The *Patagonian beds* represent an Atlantic marine transgression occurred in a wide area of Patagonia during the early Miocene (Malumíán and Náñez, 2011; Encinas *et al.*, 2018a). For the study area, Ugarte (1956) used the informal term Patagoniano to refer to the marine deposits cropping out in the Río Jeinemeni and surrounding areas. Other authors use Patagonia Formation (Lapido, 1979; Ramos, 1979; Homovc, 1980) to describe and gather all deposits with marine invertebrate remains and trace fossils. The Centinela Formation was defined near Lago Argentino (Furque and Camacho, 1972) and numerous works used this definition and extended it to all cordilleran marine Oligocene-Miocene deposits. Sedimentological studies by Cuitiño and Scasso (2010) in the southern coast of Lago Argentino, redefined marine Patagonian beds, grouping these marine deposits in the Estancia 25 de Mayo Formation (Fig. 2). Near Pueyrredón-Posadas region these marine beds are named El Chacay Formation (Chiesa and Camacho, 1995; Cuitiño *et al.*, 2015, 2019; Parras *et al.*, 2012; Fig. 2). Analyzing all stratigraphic bibliography we decided to consider the term Centinela Formation (Fig. 2) according to Escosteguy *et al.* (2003) preceded by Giacosa and Franchi (1997) who extended this terminology to the study area.

In the study area, and particularly in the western and southern border of the Lago Buenos Aires Plateau (Fig. 1), Ugarte (1956) defined the Río Zeballos Group to include all the continental Miocene deposits that cover transitionally the marine deposits. This unit is composed of a coarsening upward succession including the Río Jeinemeni, Cerro Boleadoras and Río Correntoso formations (Ugarte, 1956; Escosteguy *et al.*, 2003; Dal Molin and Colombo, 2003). Near the boundary between the Río Jeinemeni and the Cerro Boleadoras formations, Folguera *et al.* (2018) dated zircons from a tuffaceous sandstone in 16.5 ± 0.3 Ma (Fig. 2). Only in the northernmost tip of the Austral-Magallanes basin, these continental beds are grouped into the Río Zeballos Group and their equivalent is the Pinturas Formation in the eastern sector of Lago Buenos Aires Plateau (De Barrio *et al.*, 1984; Bown and Larriestra, 1990) (Fig. 2). In the rest of Austral-Magallanes Basin, the Miocene continental deposits cropping out along the Southern Patagonian Andes are referred as the Santa Cruz Formation (Feruglio, 1949; Furque, 1973; Cuitiño *et al.*, 2019) (Fig. 2).

The upper part of the Río Zeballos Group,

represented by the Río Correntoso Formation, is mainly covered by late Miocene – Quaternary basalts of the Meseta del Lago Buenos Aires Formation (Gorring *et al.*, 1997; Ton-That *et al.*, 1999; Kay *et al.*, 2002), dated from 9 Ma to 0.2 Ma (Sinito, 1980; Ramos and Kay, 1992).

The study region also roughly coincides with a two-fold segmentation of the Patagonian Cordillera since the Mesozoic, suggesting reactivation of former tectonic control along it (Suárez, 1976; Ramos, 1989; Kraemer and Riccardi, 1997; Lagabrielle *et al.*, 2004). Thermochronological data from the cordillera consistently indicate an Oligocene to Miocene deformational phase that advanced from the western basement domain towards the eastern fold and thrust belt (*e.g.* Thomson *et al.*, 2001; see Ghiglione *et al.*, 2016a for a review). These tectonic scenario produced growth strata and syntectonic unconformities (Barberón *et al.*, 2018) within the Neogene succession implying that these deposits can be considered as syndeformational. Denudation along the eastern margin of the basement domain in the Southern Patagonian Andes, registered in young apatite fission track ages, range between 9 and 4 km with ages between 14 and 5 Ma (Fosdick *et al.*, 2013) or 12–8 Ma (Thomson *et al.*, 2001; Thomson *et al.*, 2010).

Miocene's framework and correlation of related areas

In Guenguel Plateau, north of the study area (Figs. 1 and 2), no marine Miocene deposits are recognized. The succession starts with continental Miocene units that are mapped as the Río Frías, Río Mayo, Pedregoso and El Portezuelo formations (Escosteguy *et al.*, 2003). At the same latitude, south of Balmaceda town in Aysén Region in Chile, these deposits are all grouped and classified as the Oscuro Formation (Rivas *et al.*, 2015), which is interpreted as volcanoclastic, alluvial and mobile channel belts of fluvial successions (Suárez *et al.*, 2000; De La Cruz *et al.*, 2003; Quiroz and Bruce, 2010). To the west of the study area, the Guadal Plateau in Chile (Fig. 2) represents a tectonically inverted basin that preserves a Cenozoic succession similar to that studied here. The older part consists of a clastic continental succession underlying the marine Guadal Formation deposits, and representing a regressive stage related to the proto-Cordillera (ca. 30 Ma). It is observed

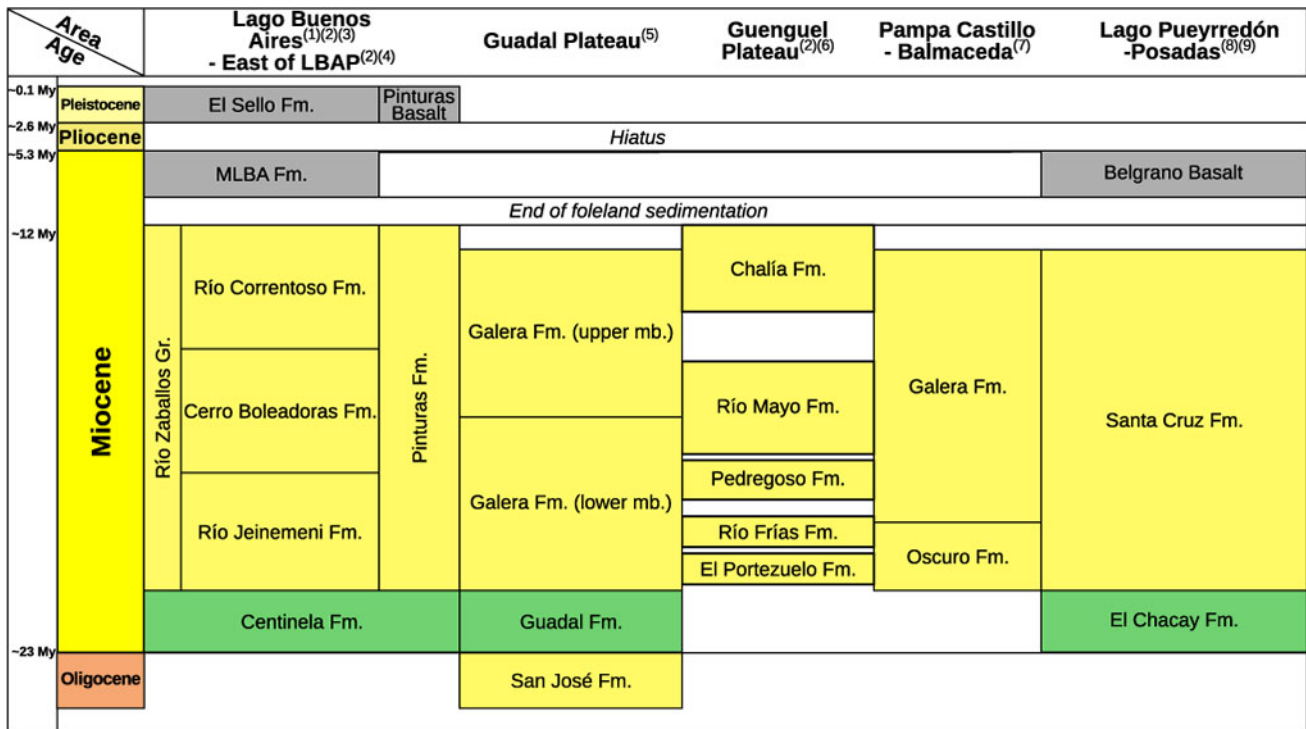


Figure 2. Stratigraphic chart for the studied units in the surrounding areas (Lago Buenos Aires, east of Lago Buenos Aires Plateau, Guadal Plateau, Guenguel Plateau, Pampa Castillo-Balmaceda and Lago Pueyrredón-Posadas). Green and yellow areas correspond to marine-transitional and terrestrial lithostratigraphic units, respectively. Grey areas correspond to basalts and lava flows. White areas correspond to hiatuses. Numbers in brackets associated to each area indicate the source of information as follows: (1) Ugarte, 1956; (2) Escosteguy *et al.*, 2003; (3) This work; (4) Bown and Larriestra, 1990; (5) Flint *et al.*, 1994; (6) Dal Molin and Franchi, 1996; (7) De La Cruz *et al.*, 2003; (8) Giacosa and Franchi, 2001; (9) Cuitiño *et al.*, 2019.

in the internal part of the Central Patagonian belt in Guadal Plateau and corresponds to the San José Formation (Flint *et al.*, 1994). Guadal Formation, deposited from Late Oligocene to Early Miocene, represents the marine deposits of the “Patagonian sea” in this tectonically inverted basin (Flint *et al.*, 1994). This marine transgression is correlated to Centinela Formation in the study area (Flint *et al.*, 1994; Encinas *et al.*, 2018a). The Guadal Formation often shows contractional syn-sedimentary deformation, such as internal thrusts and duplex systems (Scalabrino *et al.*, 2009). The equivalents of the terrestrial clastic deposits of the Santa Cruz Formation and Río Zeballos Group in Guadal Plateau are the Pampa Castillo and Galeras formations (Flint *et al.*, 1994). These units include terrestrial sandstones, claystones, and minor conglomerates (Scalabrino *et al.*, 2009; Encinas *et al.*, 2018a).

In the eastern edge of the Lago Buenos Aires Plateau, close to the Deseado Massif, no Miocene marine deposits are recognized. In this area, continental Miocene deposits are represented by

the volcanoclastic Pinturas Formation (Fig. 2) with well-developed paleosol horizons preserved (Bown and Larriestra, 1990; Escosteguy *et al.*, 2003), lying directly above Jurassic volcanoclastic deposits.

Chronostratigraphy

Sr/Sr dating of oysters as well as Ar/Ar and U-Pb tuff ages, yield ages between 22 and 18 Ma for Patagonian marine deposits of the Austral-Magallanes Basin (Parras *et al.*, 2012; Cuitiño *et al.*, 2012, 2015). In turn, available ages for the continental clastic successions indicate that the mid-section of the Río Zeballos Group (Cerro Boleadoras Fm.) deposited at around $\sim 16.5 \pm 0.3$ Ma (Folguera *et al.*, 2018). South of the study area, near Lago Pueyrredón-Posadas, the age of the Santa Cruz Formation (equivalent to Río Zeballos Group) has been constrained between 22 and 14 Ma by tuffaceous deposits (Blisniuk *et al.*, 2005), although latter Perkins *et al.* (2012) and Cuitiño *et al.* (2015) estimated its basal age around 18 Ma.

| Name | Description | Occurrence and distribution | Interpretation |
|------------|-------------------------------------------------------------------------------------------------------------------------------------------------------------------------------------------------------------------------------------------------------------------|----------------------------------------------------------------------------------------------------------------------------------------------|-------------------------------------------------------------------------------------------------------------------------------------------------------------------------------------------------------------------------------------------------------------------------------------------------------------|
| <i>Fm</i> | Massive, dark redish to gray and green mudstones. Some cases display macro pedogenic features such as rootless, blocky structures, white mottles and oxide impregnations. Isolated carbonate nodules interspersed are recognized associated with this lithofacies | Moderate occurrence, generally below medium-sandstones beds. Low occurrence but concentrated in base sector of the stratigraphic section | Deposition of clay to silt sized sediments by decantation in backswamp or abandoned channel deposits produced during floods. Pedogenesis after deposition is interpreted by pedogenic features |
| <i>Fl</i> | Horizontal laminated mudstones to silstones, red to light-green gray colour | Low to moderate occurrence, concentrated in the base section and interspersed between sandstones deposits to the top of the section | Decantation in floodplains, abandoned channel deposits or waning flood deposits during floods Deposition of silt-mudstones sediments by decantation in tranquil backswamp or abandoned channel deposits produced during floods |
| <i>Ht</i> | Massive to current ripple laminated very fine to fine sandstones with milimeter to centimeter dark-green, black, yellowish- to greenish-gray massive mudstones | Low occurrence distribution constrained to the base of the studied section. Sandstone proportion increases to the top of associated deposits | Mud-sand alternations are produced by fluctuation in the energy of the currents, which produce alternating traction and decantation processes, probably caused by tidally-modulated currents. Variation in the proportion and thickness of sand/mud ratio imply changes in sediment supplyan current energy |
| <i>Sm</i> | Massive medium-grained sandstones, moderate sorted, yellowish-gray to gray colour. Moderate occurrence | Moderate occurrence concentrated in the upper sector of the studied section | Sediment-gravity flow deposits, debris flow or channel infill collapse |
| <i>Sr</i> | Current ripple laminated very fine to fine-grained sandstones | Low occurrence concentrated in the lower parts of the studied section | Current ripples migration in a low flow regime |
| <i>Sh</i> | Horizontal stratified medium-grained sandstones, moderate sorted gray colour | Moderate occurrence distributed from mid sector to the top of the estudied section | Produced by planar bed-forms in upper flow regime |
| <i>Sp</i> | Planar cross-bedded medium-grained sandstones, well sorted gray colour | Moderate occurrence distributed from mid sector to the top of the estudied section | Migration of subaqueous dunes with linear crest in lower flow regime |
| <i>St</i> | Trough cross-bedded medium-grained sandstones, well sorted yollowish-gray to dark gray colour. Sometimes of these beds are associated with undifferentiated vertebrate remains | Very high occurrence distributed from middle to upper sectors of the studied section | Migration of subaqueous dunes with undulate crest in lower flow regime |
| <i>Sd</i> | Slightly disturbed stratification layers, moderated sorted, medium-grained sandstones, gray colour | Moderate occurrence distributed from middle to upper sectors of the studied section | Liquefaction caused by partial subaerial exposure or overloading during channel beds deposition |
| <i>Spp</i> | Planar cross-bedded medium-grained sandstones, very-well sorted reddish gray to gray colour, limited by parallel surfaces with angular base-boundary foresets in association with trace fossil <i>Celliforma</i> isp. | Very low occurrence concentrated in mid sector of the studied section | Transverse dunes with linear crest by migration in lower flow regime. Eolian-fluvial interactions features suchs as angular base-boundary and set thicknesses arround 1.5 m |
| <i>SGm</i> | Massive clast-supported, medium-grained to pebble sandstones, moderately sorted, gray colour | Low to moderate occurrence constrained to the upper portion of the studied section | Sediment-gravity flow deposits, debris flow associated deposits and sheet-floods |
| <i>SGh</i> | Horizontal stratified medium-grained to pebble sandstones, moderately sorted, gray colour | Low to moderate occurrence constrained to the upper portion of the studied section | Planar bed-form in upper flow regime |
| <i>SGp</i> | Planar cross-bedded medium-grained to pebble sandstones, moderately sorted, gray colour | Low to moderate occurrence constrained to the upper portion of the studied section | Transverse dunes with linear crest by migration in lower flow regime |
| <i>SGt</i> | Trough cross-bedded medium-grained to pebble sandstones, moderately sorted, gray colour | Moderate occurrence concentrated in the upper sector of the studied section | Transverse dunes with sinuous crest by migration in lower flow regime |

| | | | |
|------------|--------------------------------------------------------------------------------------------------------------------------------------------------------------------------------------------------------------------------------------------------------------------------------------------------------|---------------------------------------------------------------------------------------------------------------------|---------------------------------------------------------------------------------------------------------------------------------------------------------------|
| Gmm | Matrix-supported, massive, gray to dark-gray coarse-grained conglomerates | Very low occurrence and concentrated in upper portion of the section | Gravity plastic debris flow deposits with high viscosity |
| Gcm | Clast-supported, massive to poorly inverse gradation, gray to dark-gray fine to medium-grained conglomerates | Low occurrence and distribution is constrained to the top of the studied section | Pseudoplastic debris flow with internal bedload characteristics in laminar to turbulent flow regime |
| Gt | Clast-supported, trough cross-bedded, gray to dark-gray fine to medium-grained conglomerates | Very low occurrence and concentrated to the top of the section | Transverse gravel bars with linear crest by migration in channel bars in high flow regime |
| Gh | Clast-supported, planar cross-bedded to poorly clast imbrication, gray to dark-gray fine to medium-grained conglomerates with moderate occurrence | Moderate occurrence and concentrated to the top of the section. Sometimes interspersed with Sp and SGt in some beds | Longitudinal gravel bars, lag deposits, sieve deposits. Quick deposition and moderated to bad sorted scour fill |
| SB | Bioturbated medium sandstones, moderate sorted, greenish gray colour. High fossil content of diverse invertebrates and trace fossils (Gastropods, Bryozoans, Brachiopods, Pectinids, Turrillids, <i>Planolites</i> isp., <i>Skolithos</i> isp., <i>Teitichnus</i> isp. and <i>Thalassinoides</i> isp.) | Low occurrence and distribution is constrained to the base of the studied section | In-situ biogenic concentrations or partially remobilized (parautochthonous). Erosional lags or reduced clastic supply in moderate to high energy environments |

Table 1. Facies defined for the analyzed stratigraphic section in the Río Jeinemeni and Río Los Antiguos. Facies code modified from Miall, 1985.

West of the study area in Meseta Chile Chico, these clastic successions are capped by lava flows dated to 16 and 4 Ma (Espinoza *et al.*, 2005). South of Lago Buenos Aires, the sub-horizontal basaltic flows of the volcanic Lago Buenos Aires Plateau, dated at around 12 Ma (Guivel *et al.*, 2006; Boutonnet *et al.*, 2010), rest unconformably over the Río Zeballos Group, confirming that erosion and compressional tectonics ceased between 14 and 12 Ma or sediment bypassed to different areas (*e.g.* Atlantic or Pacific oceans; Lagabrielle *et al.*, 2004; Scalabrino, 2009).

METHODOLOGY

Geological fieldwork was conducted in the area in two opportunities since 2016. Geological observations in the field included measurement and facies description (Tables 1 and 2) for a sedimentary column located in the northwestern border of Lago Buenos Aires Plateau, near Los Antiguos (46° 40'S; 71° 40'W), in one of the most complete sections for the Miocene sedimentary record (Fig. 1). This section is close to that measured by Escosteguy *et al.* (2003) and Dal Molin and Colombo (2003).

Detailed observations include bed thickness and geometry, sedimentary structures and grain size. Paleocurrent directions were also registered in cross-bedded sandstones, especially in good 3D exposures

allowing the measurement of true dipping direction of cross-beds. Facies analysis and codes were undertaken following the criteria of Miall (1985).

SEDIMENTARY FACIES ANALYSIS

In order to provide a hierarchical order to the sedimentologic field data collected for the Centinela Formation and Río Zeballos Group, nineteen facies are defined (Tables 1 and 2). Those facies are grouped into eight facies associations (*Facies Association I* to *Facies Association VIII*), which in turn are grouped into three sedimentary units (*Sedimentary unit I*, *Sedimentary unit II* and *Sedimentary unit III*).

Facies association I: Bioturbated and massive sandstones

Facies association I (FA I) represents only 5% of the studied stratigraphic section and is dominated by bioturbated, greenish-gray and yellowish-gray sandstones, constituted by facies SB, grading from more to less bioturbation towards the top (Fig. 3). These bioturbated sandstone deposits are interspersed with massive sandstone beds (facies Sm) and usually reach up to 0.8 m in the lower sector of the Facies and up to 2 m near the top of the Facies. Occasionally, interspersed laminated sandy-

| Facies | Facies Association | Geometry | Dimension | | Boundary | | Assamblage Sedimentary Unit |
|---------------------------------|--------------------|------------|---------------|------------|----------|------------|-----------------------------|
| | | | Thickness (m) | Lenght (m) | Top | Basal | |
| SB, Sm, SGm, Fl | FA I | Tabular | 50 | 50 | Planar | Planar | I |
| Ht, Sr, Sm | FA II | Tabular | 70 | 30 | Planar | Planar | |
| Fm, Fl, Sm, Sh, Sp | FA III | Tabular | 20 | 30 | Planar | Planar | II |
| St, Gh, SGm, Sm, Sh, Sd, Fm, Fl | FA IV | Lenticular | 10 | 15 | Planar | Concave-up | |
| Spp, Sm, Fm, Fl | FA V | Tabular | 50 | 10 | Planar | Planar | |
| SGt, SGp, SGh, SGm, Fm | FA VI | Tabular | 10 | 30 | Planar | Planar | |
| Gcm, Gh, SGh, SGm, Gt | FA VII | Lenticular | 10 | 20 | Planar | Concave-up | III |
| Gmm, Gh | FA VIII | Tabular | 30 | 30 | Planar | Planar | |

Table 2. Hierarchical facies scheme proposed for the Neogene sedimentary section of the northwestern Austral-Magallanes Basin.

siltstones (facies Fl) layers of 0.2 m-thick are present. Bioclastic coarse sandstone beds with disarticulated shell remains are less common and are recognized to the top of the FA (facies SGm). Above this sandstone, usually an incipient 0.2 m-thick laminated sandy-siltstone (facies Fl) bed is present.

Bioturbation, characterized by horizontal and vertical burrows (e.g. *Planolites* isp., *Skolithos* isp., *Teichichnus* isp., *Thalassinoides* isp.), is common in FA I, diminishing from base to top. Marine invertebrate fossil remains as pectinids, oysters, turritellids, undifferentiated gastropods and bivalves, bryozoans and other undifferentiated shells characterize this FA (Fig. 3). FA I shows sharp contact with the overlying FA II by a marked grain size change from a bioclastic pebble-sandstone to a laminated siltstone.

Interpretation. The presence of bioturbated sandstones, massive sandstones and sandstones with marine invertebrate remains such as turritellids, pectinids, brachiopods, bryozoans among others, allows interpreting FA I as deposited in a coastal marine environment. The medium-grained sandstones showing an aggradational stacking pattern with interbedded laminated sandy siltstones, suggests that incipient bathymetric changes occurred, indicating deposition in a coastal

marine to transitional continental environment. Sandstone deposits with reworked fossils remains, indicates high-energy events, probably due to wave influence. The diminishing of bioturbation towards the top of this FA I, and the gradation to lamination-dominated facies, indicates a subtle bathymetric decrease, probably produced by stressing environmental conditions for marine life (Taylor and Goldring, 1993). The presence of a disarticulated and fragmented shell-bed in the upper part of FA I indicate an event of moderate energy that reworked the invertebrate fauna (Kidwell *et al.*, 1986) and culminates in a bioclastic pebble-sandstone.

Facies association II: Heterolithic deposits

Facies association II (FA II) represents 8% of the studied stratigraphic section and is dominated by heterolithic deposits (Fig. 4) reaching up to 70 m thick, corresponding to a centimeter- to millimeter-thick alternation of greenish-gray sandstone, siltstone and dark green mudstone. These are arranged from base to top in lenticular, wavy and flaser heterolithic (facies Ht) bedding patterns. Sandstone and coarse-grained siltstone layers usually reach a thickness of 0.2 m and usually display current ripples (facies Sr), parallel lamination or be massive (facies Sm). FA II culminates in a clearly recognizable massive

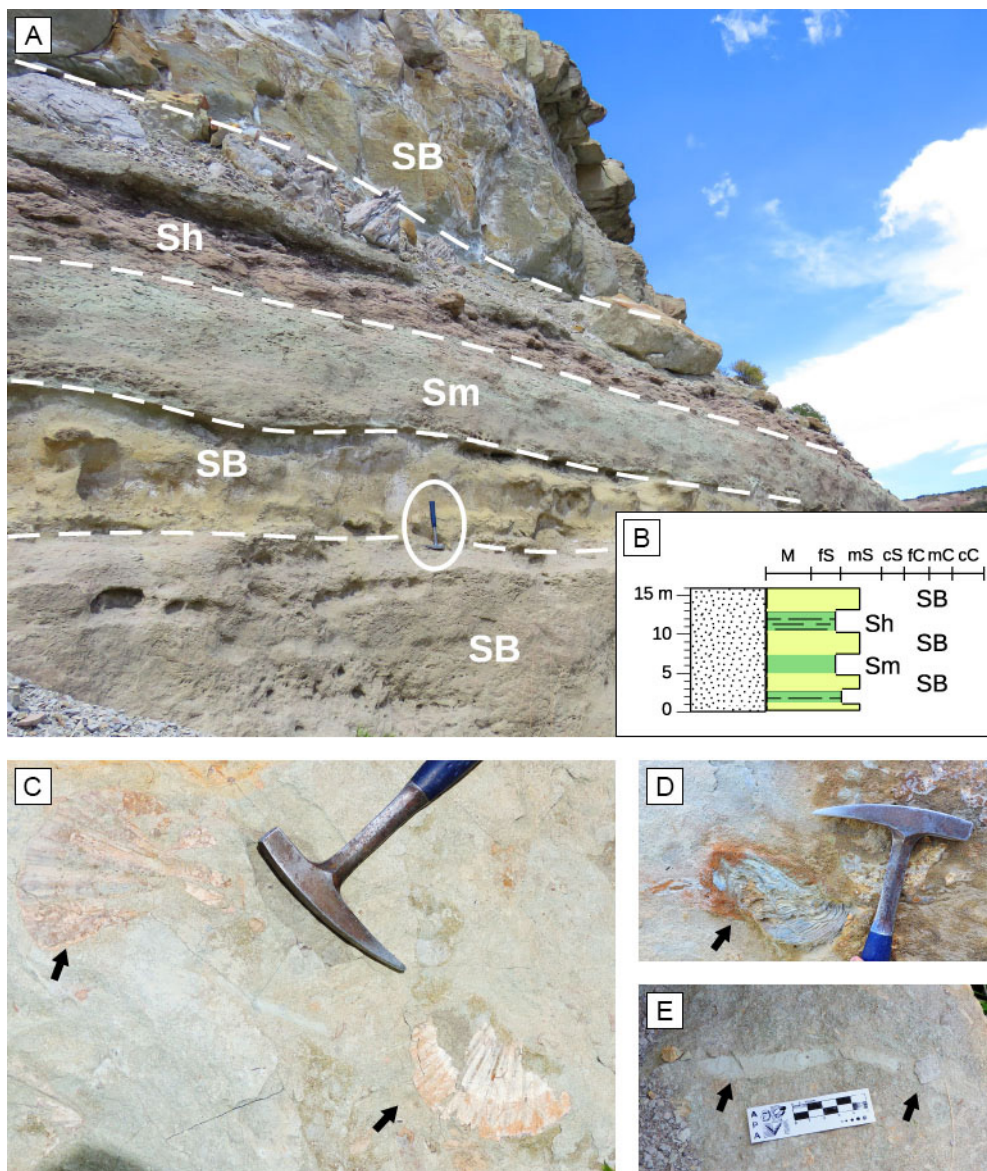


Figure 3. Outcrop pictures and stratigraphic section model for the FA I (Centinela Formation) along the margins of Río Jeinemeni. **a)** General outcrop view of FA I. A decreasing in bioturbation activity is identified to the top of the sandstone beds. **b)** Stratigraphic section model for FA I. **c)** Detail of Pectinids marked by the black arrows. **d)** Detail of Oyster remains indicated by black arrow, mostly preserved in basal portion of FA I. **e)** Horizontal burrows immersed in medium-sandstone and infilled with fine- to very-fine sandstones (black arrows). In pictures a), c) and d) hammer for scale (40 cm).

greenish gray to gray massive sandstone (facies Sm) that reach up to 10 m thick. The absence of bioturbation is the diagnostic feature of FA II.

Interpretation. The abundance of heterolithic deposits displaying different mix-layers patterns (Reineck and Wunderlich, 1968) and current ripple lamination suggest tide-modulated currents (Cuitiño *et al.*, 2015). The absence of bioturbation along this facies indicates a stressed marine paleoenvironmental condition to biota influence (Taylor and Goldring, 1993; Cuitiño *et al.*, 2015). The presence of massive tabular sandstone deposit at the top of the FA could be interpreted as shallow marine beach on an open-wide coastal environment receiving moderate energy

(Cuitiño *et al.*, 2015). The lack of bioturbation and fossil remains contradict the interpretation of open marine conditions. Stratigraphic relations between FA I and FA III (see below) imply that for FA II still prevail the transitional marine environments. In this way, the heterolithic deposits of FA II are interpreted as tidal flat environment. The absence of paleosol horizons is additional evidence supporting this interpretation.

Facies association III: Structureless to laminated mudstones with incipient pedogenic features

This Facies association (FA III) represents 15% of the measured section and is mostly concentrated

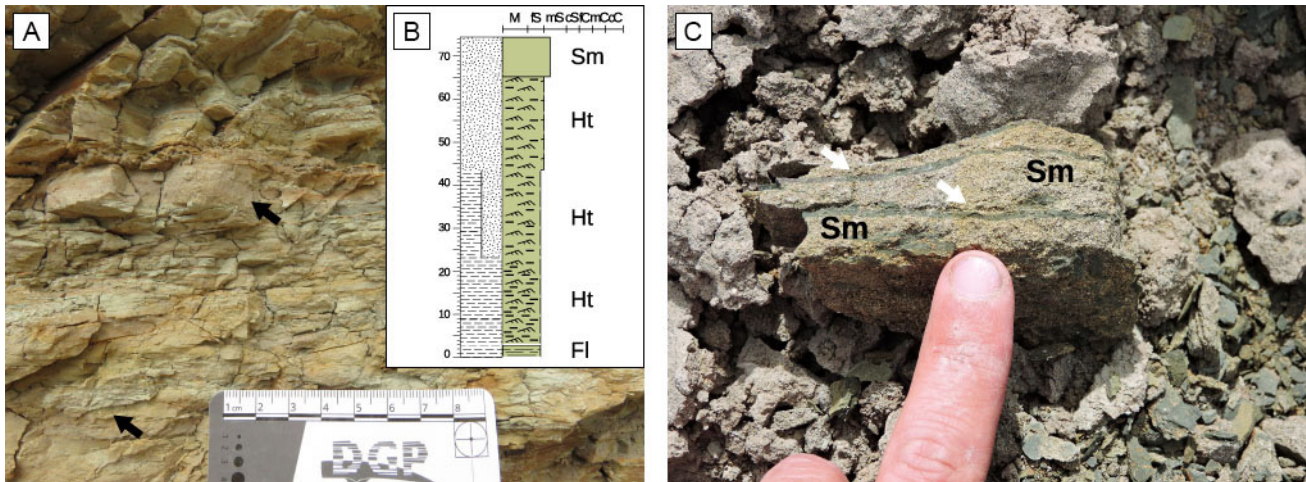


Figure 4. Horizontal heterolithic yellowish to greenish deposits of FA II and stratigraphic section model. **a)** Basal section of this FA where lenticular heterolithic deposits dominate (facies Ht). Millimeter- to centimeter-thick sandstone layers (black arrows, facies Sm or Sh) intercalate with mudstone layers (facies Fm). **b)** Stratigraphic section model for FA II. **c)** Detail of the top of FA II where greenish fine to very fine sandstones dominate (facies Hf), note the presence of millimeter- to centimeter- mudstones layers (white arrows).

in the Río Jeinemeni Formation. It is dominated by massive mudstones (facies Fm) with centimeter-thick interbedded dark-red to greenish fine laminated mudstones (facies Fl) and massive yellowish-gray sandstones (facies Sm; Fig. 5). In outcrops this FA is clearly recognized by the “*bad-land*” landscape. Beds are tabular and vary in thickness from some meters up-to 20 m. Some centimeter-thick laminated mudstones (facies Fl) are visible sometimes interbedded between the massive mudstones (facies Fm; Fig. 5). Macro pedogenic features such as root traces, blocky structures, slickensides and Fe-oxide mottles are recognized in FA III (facies Fm; Fig. 5). In some vertical exposures, coloration changes of fine-grained levels suggest changes in the composition of mudstones. Carbonate nodules are observed locally in certain mudstone layers as well as desiccation cracks. Tabular yellowish-gray to gray fine-to-medium-grained massive sandstone (facies Sm) are interbedded with mudstone deposits, ranging in thickness from a few decimeters to up to 1 m. They show sharp planar bases (Fig. 5) and they are more common in the Cerro Boleadoras Formation. In addition, some lenticular isolated sandstone beds show planar base and convex-up top (*i.e.* lobe-shape geometries) and internally are characterized by structures such as planar cross-bedding (facies Sp) and horizontal bedding (facies Sh). Some syn-sedimentary deformation is developed in these fine-grained deposits.

Interpretation. The dominance of massive mudstones and the relative scarcity of interspersed massive sandstones indicate deposition in a low-energy, low gradient environment, punctuated by some non-depositional episodes developing incipient pedogenic features such as fluvial floodplains (Miall, 2006). Recognition of interspersed dark-red and light-green colors in fine-grained deposits of FA III can be interpreted as changes in the iron oxidation state (redox state) promoted by variations in the drainage conditions of paleosols (Retallak, 2001; Kraus, 1999). Massive sandstone sheets indicate the action of tractive currents which can be interpreted as initial stage of flooding episodes, producing unconfined flows on the floodplain (Miall, 1988; Mjøs *et al.*, 1993; Viseras *et al.*, 2018). The occasional presence of lobe-shaped wedges of fine-grained sandstones with horizontal bedding or planar stratification are interpreted as crevasse splays produced after channel margin surpass during flood stages implying fast sedimentation episodes (Miall, 1985; 1988). The close relation between FA III and FA IV (see below) supports the interpretation of FA III as a floodplain and crevasse-splay deposits.

Facies association IV: Lenticular cross-bedded medium- to pebble-grained sandstones

This Facies association (FA IV), representing the 33% of the stratigraphic column, is the most

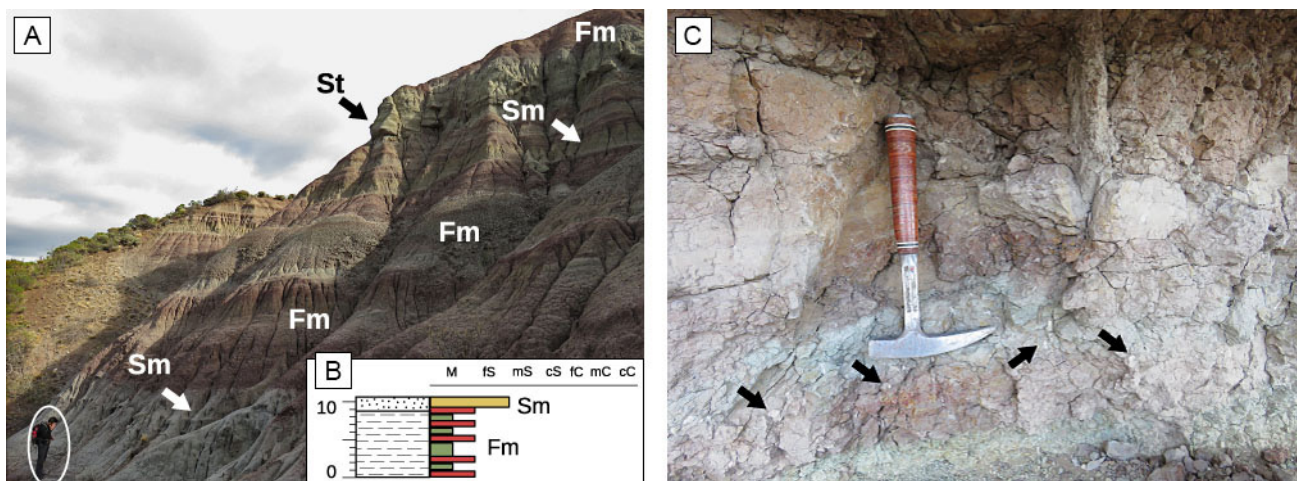


Figure 5. Sub-horizontal to horizontal greenish to reddish mudstones of FA III. **a)** Characteristic “bad land” landscape of this FA. The interspersed yellowish-gray massive sandstones (facies Sm) project off the outcrop. To the top of the picture a thicker cross-bedded sandstone (facies St) is visible. **b)** Stratigraphic section model for FA III. **c)** Detail of alternate greenish to reddish mudstones with pedogenic features such as rootless, blocky structures, white mottles and oxide impregnations (facies Fm). Carbonate nodules (black arrows) and the intercalation of centimeter massive mudstone are shown. In picture c) hammer for scale (40 cm).

extended in all outcrops visited and dominates in the Cerro Boleadoras Formation.

FA IV is mostly composed of lenticular concave-up to tabular bodies of reddish-gray to yellowish-gray sandstones (facies St) with sharp base and homogenous grain-size (Fig. 6), although fining-upward trends are evident. Grain-size is mostly medium-grained sandstone at the bottom which grade towards the top to fine- to very fine-grained sandstones (fining-upwards trend) or occasionally to coarse to pebble-grained sandstones (coarsening-upwards trend) to the top. Some minor thin pebble-grained sandstones or fine-grained conglomerates with horizontal stratification (facies Gh) are present at the base of the beds (Fig. 6). In some sandstone bodies, a thin basal-lag of mudstone intraclasts is observed covering the bottom surface (facies SGm). Thicknesses of sandstone bodies is commonly ~10 m, but it can vary between 3 to 14 m. Internal erosion surfaces are rarely observed, although the thicker bodies show internal reactivation surfaces covered by thin layers of coarse-to-pebble sandstones. From base to top, sedimentary structures within FA IV bodies are arranged as horizontal stratification (facies Sh), trough cross-bedded coarse-grained sandstones (facies St), and massive sandstones (facies Sm) or massive to laminated mudstones (facies Fm and Fl). Occasionally, massive sandstones are crowned by medium-grained trough cross-

bedded sandstones in sharp erosive contact. These particular sandstone bodies are interbedded with another common arrangement characterized by an incipient coarsening-upwards medium- to coarse-grained sandstones bodies with mainly trough cross-bedded stratification (facies St) and sharp erosive basal boundary. Internal reactivation surfaces covered by thin-bedded layers of coarse-to-pebble-grained sandstones are common in these bodies. Usually deformational structures (facies Sd) are developed on cross-stratified medium-grained sandstones. Wings are observed towards the lateral limits of the bodies of FA IV, wedging-out into fine-grained floodplain mudstones deposits (FA III). Few manifestations of vertebrate remains such as skulls, Glyptodon plates and undetermined long-bones, are dispersed in these deposits. Paleocurrent measurements in trough cross-bedded sandstones cluster in a NE-SW direction with no remarkable tendency through the stratigraphic section but a mean paleocurrent direction to the E. Some syn-sedimentary deformation is developed in these medium-grained deposits interbedded with fine-grained deposits of FA III.

Interpretation. Lenticular sandstone bodies isolated within floodplain deposits (FA III) are interpreted as fluvial channel deposits. The internal cross-bedded sandstones, the fining upward trend and

the erosive concave-up base are also indicative of channel deposition (Miall, 1985). Given the simple infill of the channels and the general reduced thickness of individual bodies, most are interpreted as shallow, single story channels (Gibling, 2006). Internal erosion surfaces observed for some thicker bodies, suggest reactivations of multistory channels (Bridge and Mackey, 1993; Gibling, 2006). At the base of the Cerro Boleadoras Formation channel bodies are commonly observed isolated within floodplain deposits whereas channel amalgamation is observed to the top of the unit. The lack of evidences for lateral accretion surfaces suggests that these were fixed channels in a low sinuosity fluvial system (Miall, 2006). These channels remain stable confined by levees and can grow vertically (Miall, 2006; Cuitiño *et al.*, 2019). The occasional presence of deformed cross-stratified sandstone layers within channel bodies is produced by liquefaction caused by sedimentary overloading or seismic triggered by the proximity of the deformational front (Van Loon, 2009; García-Tortosa *et al.*, 2011). There is a clearly interbedding relation between FA IV representing the fluvial channels and FA III floodplains related to those channels (Miall, 1988; 2006).

Facies association V: Well sorted, large-scale trough cross-bedded sandstones

Facies association V (FA V) represents less than 5% of the column and is dominated by very well sorted medium-grained sandstones developed in the middle section of the Cerro Boleadoras Formation. This FA is mostly composed by tabular bodies of trough cross-bedded reddish-gray to gray sandstones (facies St) with sharp base contact (Fig. 7) and planar to tangential trough shaped foresets (facies Spp). The mean-thickness of sandstone bodies is 14 m. Internally, cross-bedded sets vary from 1 to 5 m with mean-thickness set of 3 m. Major erosion surfaces are rarely observed in these sandstone-bodies, although are limited by mostly parallel surfaces with angular base-boundary foresets. FA V bodies are interbedded with massive very fine-grained sandstones (facies Sm) or massive to laminated mudstones (facies Fm and Fl); sometimes associated with isolated barrel to oval-shaped bee cells trace fossil. Occasionally, massive mudstones show macro pedogenic features such as blocky structures and white mottles or nodules.

Interpretation. Well sorted sandstones arranged in large-scale trough cross bedded sets, suggest an aeolian origin probably by means of dune migration (Walker and James, 1992; Brookfield and Ahlbrandt, 2000). The presence of horizontal and sharp upper and lower boundary surfaces of these deposits, suggest that these surfaces could be related to deflation processes down to the water table (Veiga *et al.*, 2002). These surfaces can also represent bypass surfaces promoted by a reduction in the angle of climb of the aeolian bedforms (to zero) due to water-table control (Kocurek and Havholm, 1993). The occurrence of isolated bee cells assigned to *Celliforma* isp. suggests an arid to semi-arid environment (Krapovickas, 2012; Zapata *et al.*, 2016). The occasional appearance of massive to laminated mudstones layers suggests a flooded interdune unit with fluvial interaction. This interaction is related to humid interdunes with a change in relative humidity towards the roof of these deposits (Langford and Chang, 1989; Herries, 1993; Veiga *et al.*, 2002).

Facies association VI: Tabular, cross-bedded very coarse- to pebble-grained sandstones

This Facies association (FA VI), dominated by pebble-grained sandstones to fine-grained conglomerates, are the second most abundant, representing the 23% of the studied column. They are frequently found interbedded with other deposits such as clast-supported to massive fine- to medium-grained conglomerates to the top of the section.

FA VI is mostly composed of tabular bodies of trough cross-bedded dark-gray pebble-grained sandstones (facies SGt) (Fig. 8) with incipient fining upward trends of 0.2 m set thickness. Planar sharp bases and tops characterize most of these tabular deposits, although some sandstones bodies show a concave-up basal boundary surfaces. Internally, these bodies display fining-upwards trend from coarse- to pebble-grained sandstone at the base to medium-grained sandstone towards the top. Mudstones are also present in some particular places as thin lenses interbedded between sandstones bodies (Fig. 8). Some minor, thin (0.3 – 0.5 m thick), fine-grained conglomerates are present at the base of the beds (Fig. 8). Thicknesses of the sandstone bodies varies from 2 to 10 m, whereas the most common thickness is 7 m. Vertical facies succession of FA VI from base to top are horizontal pebble-grained sandstone

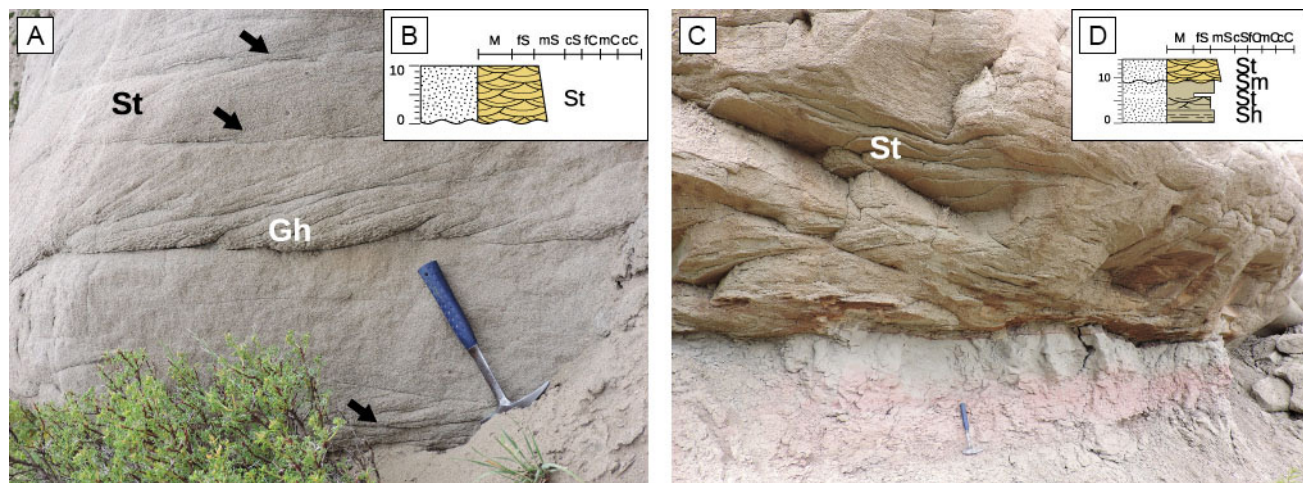


Figure 6. Sub-horizontal gray cross-bedded sandstones beds of FA IV. Two different internal arrangements are developed and also a stratigraphic section model for each one is displayed. **a)** Characteristic channel deposit arrangement for the basal and top of Cerro Boleadoras Formation showing trough cross-bedded sandstone beds (facies St), internal reactivation surfaces (black arrows), covered by thin layers of coarse-to-pebble sandstones (facies Gh) and also a basal thin-conglomerate with horizontal bedding (facies Gh). **b)** Stratigraphic section model for the first internal arrangement of FA IV. **c)** Characteristic channel deposit arrangement intercalated in the mid-section of Cerro Boleadoras Formation, composed of thinner cross-bedded sandstones. Also some deposits of FA III underlying. To the top of the outcrop medium trough cross-bedded sandstones in sharp erosive base contact is developed. **d)** Stratigraphic section model for the second internal arrangement of FA IV. In pictures b) and d) hammer for scale (40 cm).

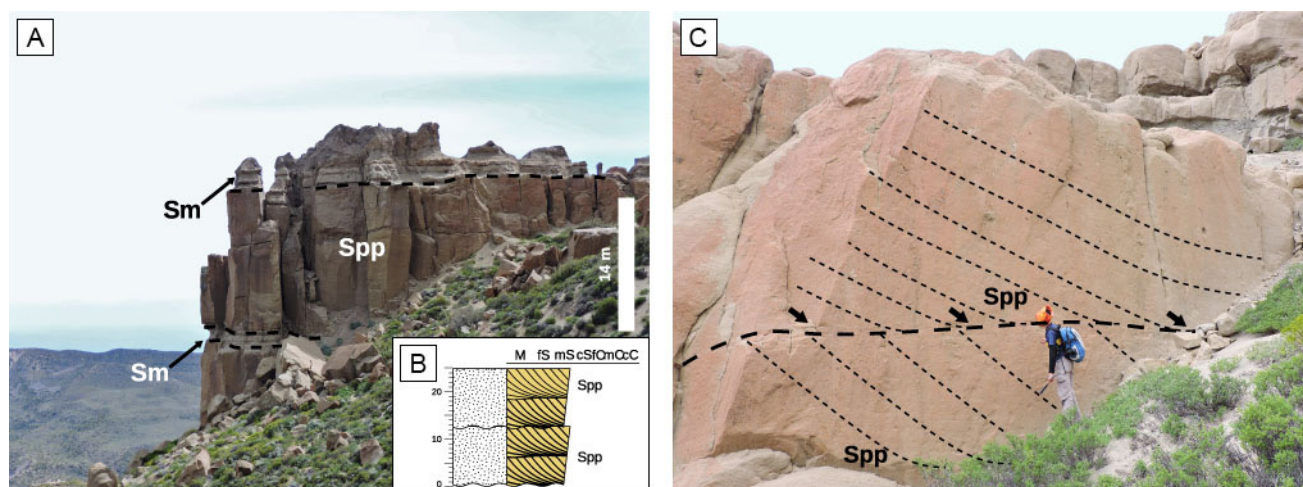


Figure 7. Horizontal reddish sandstones beds of FA V. **a)** General view of tabular, very-well sorted, trough cross-bedded sandstones (facies Spp), interspersed with massive gray sandstones of FA VI. **b)** Stratigraphic section model of these beds very well sorted sandstones. **c)** Detail of tabular sandstone bodies. Note the 3 m-thick sandstone set (person as scale of 1,6 m). Dashed line marks the parallel surfaces with angular base-boundary foresets (black arrows).

stratification (facies SGh), trough cross-bedded pebble-sandstones (facies SGt) and planar cross-bedded coarse- to pebble-grained sandstones (facies SGp). In some cases a thin centimeter to meter-thick massive mudstones (facies Fm) layer are interbedded or covering the SGp facies. This facies succession is more frequent in the middle part of the Río

Correntoso Formation. To the base of Río Correntoso Formation very coarse- to pebble-grained sandstones bodies of this FA are characterized by tabular internal trough-cross bedding (SGt) with planar base and top boundary surfaces. To the top of the section, FA VI change its internal arrangement towards simply massive pebble-sandstones (facies SGM).

Interpretation. Tabular sandstone bodies with tractive bedload sedimentation are interpreted as sheet-flood deposits (Overeem, 2004). The internal cross-bedded sandstones, the fining upward trend and the planar base and in some cases erosive concave-up base boundary are indicative of unconfined channel beds sedimentation environment (Overeem, 2004; Bridge and Demicco, 2008; North and Davidson, 2012). Given the complex infill of the sheet-floods deposits most are interpreted as shallow sporadic flooding episodes crevasse splays. These deposits are commonly dominated by trough cross-bedded, planar cross-bedded and horizontal stratification as a result of different fluvial processes such as: suspension, bedload and loosing volume downslope through infiltration of water (Reading and Collinson, 1996; Overeem, 2004; Bridge and Demicco, 2008). These lobes with sharply defined base contact tend to develop during the earliest stages of a flood event (Wasson, 1974). At the base of the Río Correntoso Formation sheets-floods deposits are characterized by very coarse cross-bedded sandstones bodies, while to the top pebble-sandstones tabular bodies dominate and only from time to time mudstones are interspersed between sandstones sheets (Miall, 1977; Heward, 1977; Nielsen, 1982). The appearance of mudstone layers indicates a diminishing in the depth of channels by the decrease of the flow energy. Base to top changes observed in these sheet-floods deposits could be related with shifts in sediment supply and accommodation space. FA VI is related and interbedded with FA VII, and to the top of the stratigraphic section with FA VIII in a different paleoenvironment (see Section 5).

Facies association VII: Clast-supported fine- to coarse-grained conglomerates

This Facies association (FA VII), representing only 7% of the stratigraphic column, is dominated by clast-supported conglomerates (facies Gcm), which appear mainly in the Río Correntoso Formation. FA VII is dominated by lenticular concave-up to tabular bodies of dark gray conglomerates with horizontal stratification (facies Gh), showing sharp-erosive basal contacts (Fig. 9) and incipient coarsening upwards trends. Thicknesses of the conglomerate bodies vary from 2 to 10 m but the most common thickness is 7 m. Sedimentary structures within these bodies are usually arranged as basal horizontal stratification

(facies Gh), occasionally trough cross-bedded fine-grained conglomerates (facies Gt), usually followed by massive fine-grained conglomerates (facies Gcm). Grain-size is mostly fine-grained conglomerate at the base and may grade to medium-grained conglomerates at the top. Some minor thin pebble-grained sandstones (facies SGh) are interspersed in FA VII bodies. Thin lag of mud rip-up clasts are observed covering the bottom surfaces (facies SGM).

Interpretation. Lenticular conglomerate bodies of FA VII interbedded with sheet-flood deposits of FA VI are interpreted as gravel-dominated channels (Viseras and Fernández, 1994; Reading and Collinson, 1996; Overeem, 2004; Bridge and Demicco, 2008; North and Davidson, 2012). The internal horizontal stratification, the coarsening upward trend and the erosive concave-up base are also indicative of channel deposition with some prograding effect in high energy fluvial systems (Miall, 1977; Sohn *et al.*, 1999). Given the simple infill of the channels and the general reduced thickness of individual bodies, most are interpreted as deep fluvial channel that allow the migration of fine-grained gravel bars followed by massive medium-grained clast-supported conglomerates remaining channel deposits (Overeem, 2004; Bridge and Demicco, 2008). Internal intercalation of sporadic pebble-sandstones and fine-grained conglomerates at the bottom of these deposits are interpreted as channel lags or lags in internal bar deposits (Walker and James, 1992). At the base of the Río Correntoso Formation these deposits are massive with incipient clast-imbrication. These channels remain mostly unstable, taking part in a high-energy fluvial system of mixed load (Schumm, 1981; Miall, 1988, 2006).

Facies association VIII: Structureless matrix-supported coarse-grained conglomerates

Facies association VIII (FA VIII), representing 5% of the stratigraphic column, is dominated by matrix-supported conglomerates at the top of the Río Correntoso Formation. It is composed mostly of tabular bodies of massive sandy to muddy-sandy matrix-supported gray to dark-gray conglomerates (facies Gmm) with sharp planar basal surface and chaotic internal arrangement (Fig. 10). Incipient coarsening upwards trend is evident, as well as inverse gradation in some conglomerate bodies.

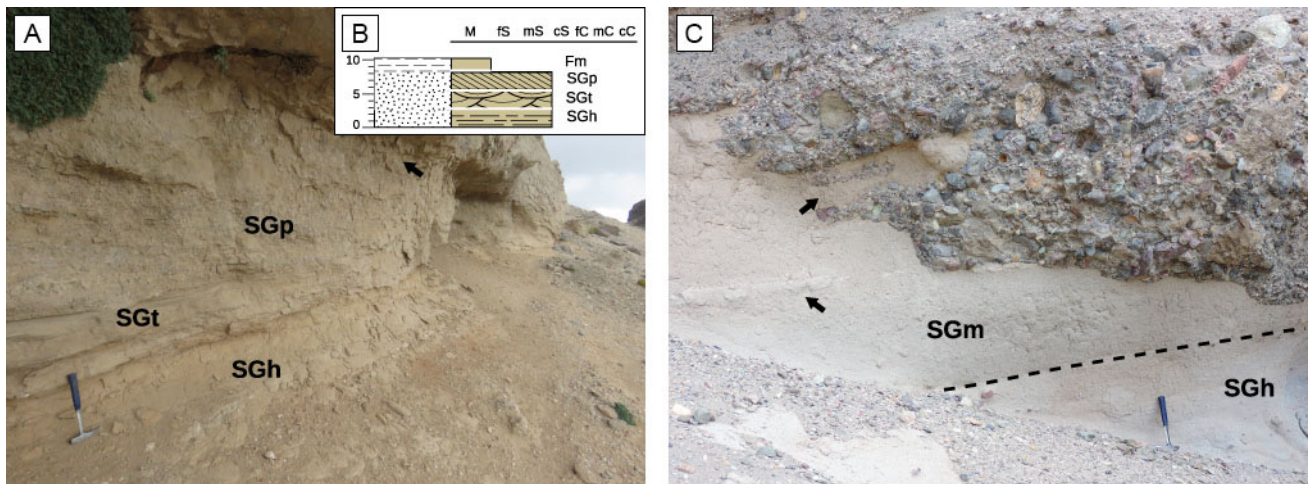


Figure 8. Pictures of outcrops and the stratigraphic section model of FA VI. **a)** Tabular bodies of horizontally stratified dark-gray pebble-sandstones (facies SGh), followed by trough-cross bedded and planar cross-bedded coarse- to pebble-sandstones (facies SGt and SGp, respectively), crowned by interspersed massive mudstones layers (facies Fm, black arrow). **b)** Stratigraphic section model for FA VI. **c)** Other typical internal arrangement of FA VI, showing horizontally stratified dark-gray pebble-sandstones (facies SGh), followed by massive gray coarse to pebble-sandstones beds (facies SGm). Black arrows mark the interspersed massive mudstones layers. To the top of the section a coarse-conglomerate with sharp erosive concave-up usually crowned these deposits of FA VI. In pictures a) and c) hammer for scale (40 cm).

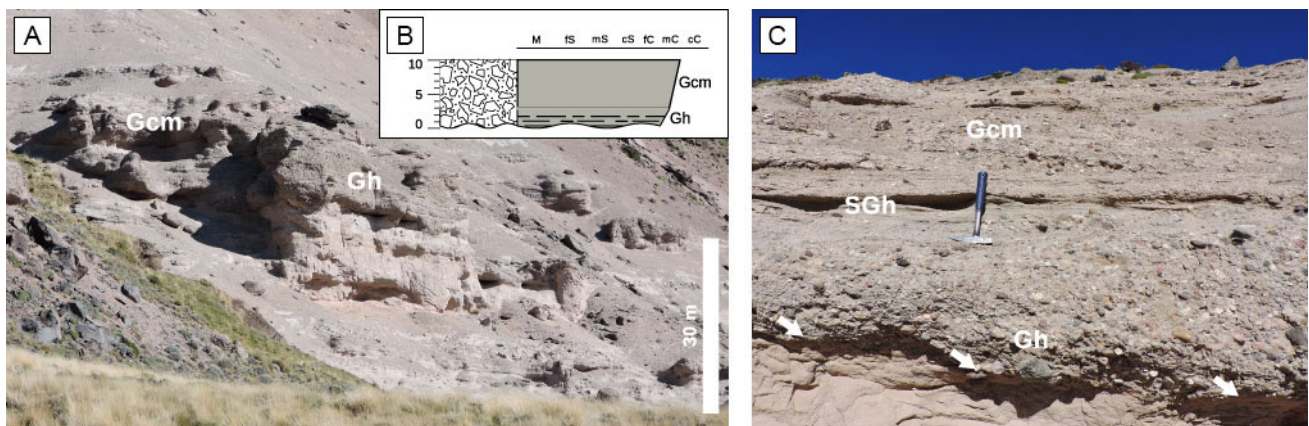


Figure 9. Pictures of outcrops and stratigraphic section model of FA VII. **a)** General aspect of FA VII where some lenses of stratified conglomerates are marked by facies Gcm and Gh. **b)** Stratigraphic section model for FA VII. **c)** Detail of a lenticular to tabular coarse conglomerate bed with horizontally stratified dark gray conglomerates (facies Gh) and interspersed pebble-sandstones with horizontal stratification (facies SGh), crowned by coarse clast-supported massive conglomerate (facies Gcm). White arrows indicate the concave-up erosive sharp contact with the underlying FA VI. In picture c) hammer for scale (40 cm).

Grain-size varies between 5 and 40 cm but the most common grain-size is 10 cm (boulder gravel). At the base of the deposits a concentration of very coarse sand to pebble grains is evident and sometimes grade to fine- to medium- boulder clasts at the top. Some minor thin fine-grained conglomerates (facies Gh) are present and in some sectors sandstones bodies developed and interspersed within the beds. The matrix is composed mostly of coarse- to medium-

grained sand, whereas sandy-muddy mixture is occasionally developed. Thicknesses of the sandstone bodies vary from 7 to 15 m but the most common thickness is 7 m. This FA is closely related and interspersed in sharp planar contact with FA VI.

Interpretation. Tabular, massive and chaotic matrix-supported conglomerates with sharp planar base and top are interpreted as debris-flow deposits

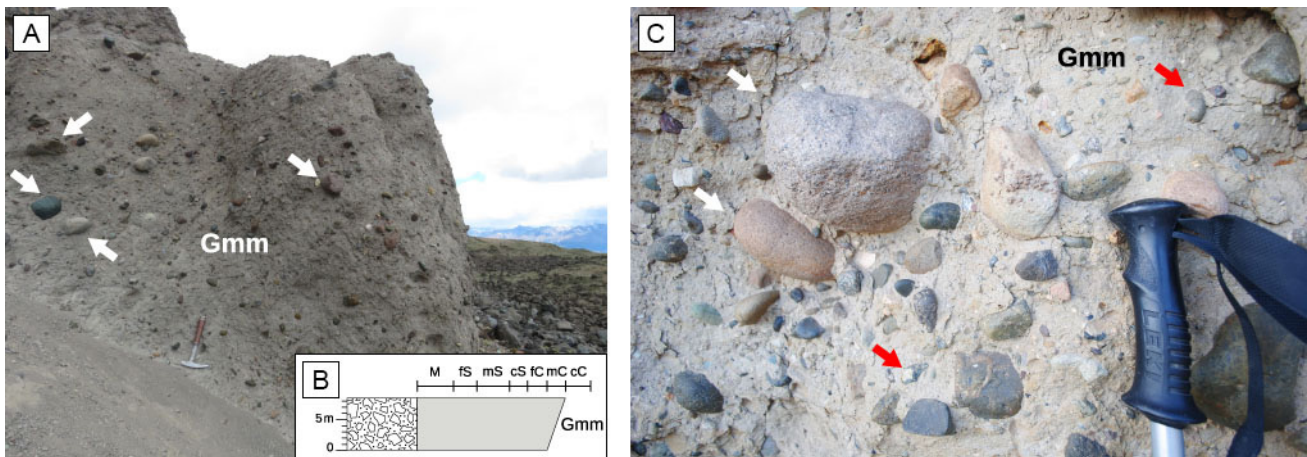


Figure 10. Pictures of outcrops and stratigraphic section model of FA VIII. **a)** General aspect of tabular and massive matrix-supported, gray to dark-gray conglomerates (Gmm). White arrows marked the most large boulder clasts (10 cm). Note hammer as a scale (40 cm) **b)** Stratigraphic section model for FA VIII. **c)** Detail of this conglomerate where fine- to medium- boulders (white arrows) and coarse pebble grains (red arrows). Note the chaotic general internal arrangement of these coarse deposits and the top of the trekking stick for scale (15 cm).

(Miall, 1977; Sohn *et al.*, 1999). The lack of muddy sediments in the matrix could be interpreted as a non-cohesive gravity flow. The internal incipient inverse grading pattern indicates an episode of pseudoplastic clast-rich debris flow that losses water content downwards (Miall, 1985; 1988; 2006; Reading and Collinson, 1996). The association of this FA with sheet-floods deposits of FA VI suggests an interaction between debris-flow deposits with sporadic flooding episodes.

SEDIMENTARY UNITS AND TEMPORAL PALEOENVIRONMENTAL EVOLUTION

Considering the stratigraphic relations and distribution of the eight Facies associations herein defined, we grouped them into three Sedimentary Units, each representing a different paleoenvironment.

Sedimentary Unit I: Shallow marine deposits

Sedimentary Unit I (SU I) is exclusive of the lower part of the studied section and compose the 13% of the whole stratigraphic section. It corresponds to the Centinela Formation, and includes FA I and FA II, which we consider genetically related because of their similar fossil content and the gradual passage between them (Fig. 11). The abundant invertebrate and trace fossil content (e.g. *Planolites* isp., *Skolithos*

isp., *Teichichnus* isp., *Thalassinoides* isp.), together with the sandy nature of the sediments in FA I, suggest accumulation in an open, shallow marine, well-oxygenated and agitated environment, with some wave-influence marked by the accumulation and reworking of fossils remains. The gradual passage to the heterolithic deposits of FA II suggests an upward shallowing of the coastal setting. The lack of bioturbation in heterolithic deposits of FA II suggests a stressing environment to biological activity probably related to subaerial exposure and/or freshwater influence. These heterolithic deposits suggest tide-modulated currents and were probably deposited in a tidal flat. Tabular sandstone deposits at the top of the FA II may provide a sign of marine beach environment receiving moderate wave energy (Cuitiño *et al.*, 2019).

Sedimentary Unit II: Mixed-load fluvial deposits

Sedimentary Unit II (SU II) represents the 53% of the studied section, forming the main depositional system for the Río Jeinemeni and Cerro Boleadoras formations. This SU includes FA III, FA IV and FA V, which are considered genetically related because of their recurrent interbedding and gradual passage between each other, suggesting this is produced by autocyclic environmental shifts (Walker and James, 1992; Reading and Collinson, 1996; Miall, 2006). The mud-dominated fluvial floodplain deposits of FA III,

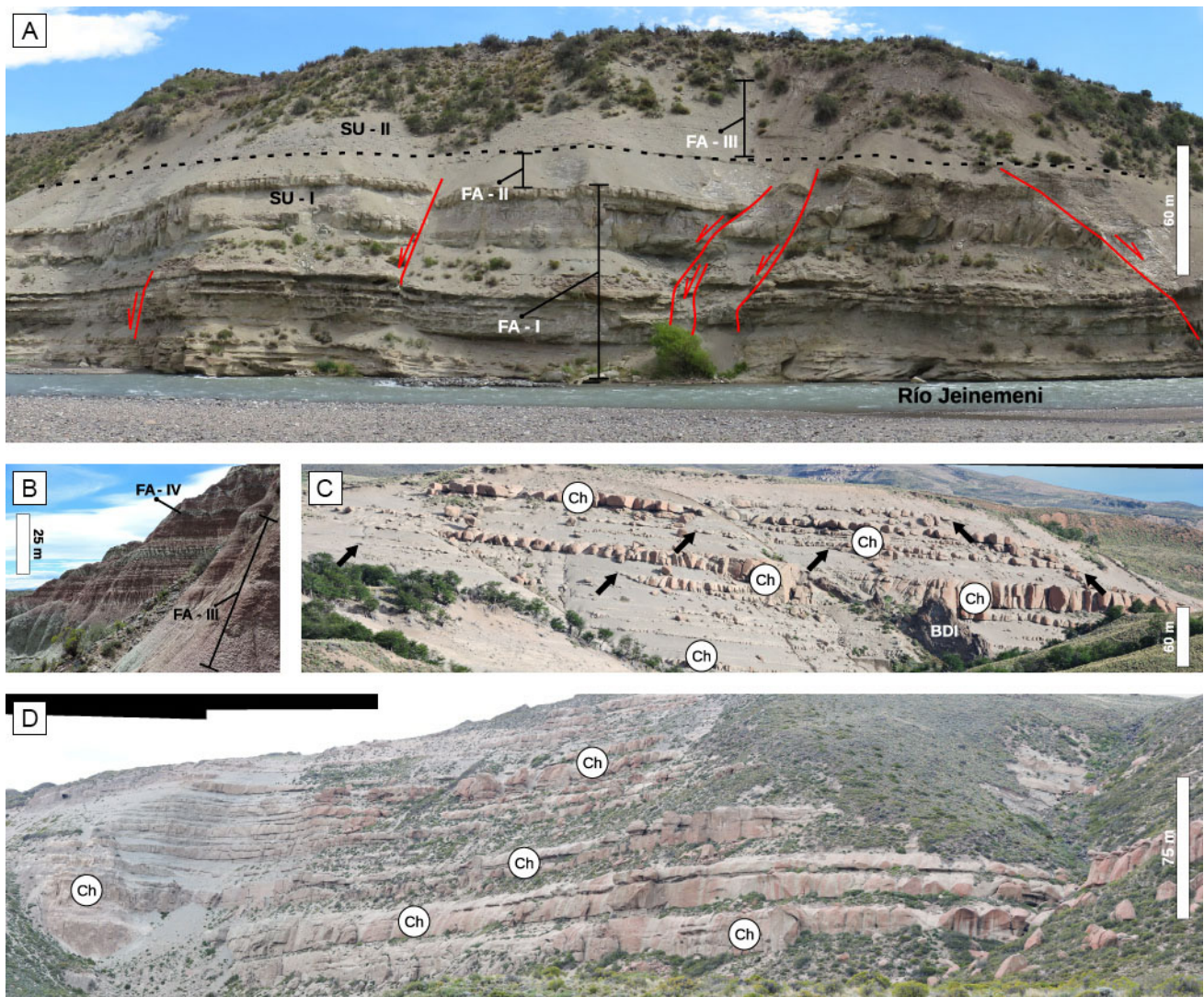


Figure 11. Outcrop views of the Sedimentary Units defined in this work that depicts the changing in accommodation space and increasing of sandstone beds proportion. **a)** General aspect of Sedimentary Unit I (SU I) and their transitional passage to Sedimentary Unit II (SU II) depicted by the dashed line. FA I and FA II, as well as some floodplain deposits of FA III, are highlighted. Red lines are drawing the structures developed after the deposition of the sedimentary units **b)** Bad lands formed in an outcrop of FA II. FA III and FA IV passage are indicated. **c)** Alternating channel and floodplain deposits from FA III and FA IV, respectively. In some cases the channel deposits are encapsulated in floodplain deposits and avulsion deposits can be detected (black arrows show the channel wings). **d)** A large scale outcrop view of SU II. Here the channel deposits are tabular, showing large lateral continuity. Note the reduction in the proportion of floodplain deposits which are mainly composed of sandstones. Ch: lenticular fluvial channel deposit.

showing macro-paleopedofeatures (Retallak, 2001; Kraus, 1999, Fig. 11), usually encapsulate some massive sandstones bodies representing crevasse splay deposits produced during flooding episodes (Miall, 1985; 2006). The alternation of floodplains (FA II) and sandy channels (FA IV) deposits indicates autocyclic processes within the fluvial system (Walker and James, 1992; Reading and Collinson, 1996; Overeem, 2004; Bridge and Demicco, 2008;

Varela *et al.*, 2012). The very well sorted sandstones of FA V, deposited in a fluvial-aeolian sedimentary system, suggest the occurrence of an isolated episode of aridification related with an allocyclic control (Miall, 1988; Reading and Collinson, 1996; Bridge and Demicco, 2008), preserved in the mid-section of the Cerro Boleadoras Formation. The lack of lateral migration surfaces within channel deposits indicates a low sinuosity fluvial system. In

turn, the intercalation of sandy channel and muddy floodplain deposits suggest this was a mixed-load fluvial system (Schumm, 1981; Miall, 1988, 2006).

Large-scale vertical changes can be recognized for the fluvial deposits of SU II. The Río Jeinemeni Formation show dispersed, small fluvial channels isolated within floodplain deposits. Upward, toward the Cerro Boleadoras Formation, channelized deposits dominate and increase their thickness, indicating a reduction in accommodation space that produce an amalgamation of channel bodies and a reduction in the proportion of floodplain deposits (Wright and Marriot, 1993; Shanley and McCabe, 1994).

Sedimentary Unit III: alluvial fan deposits

Sedimentary Unit III (SU III) represents 33% of the section and is the main depositional setting of the Río Correntoso Formation. It includes the coarsest deposits as well as some sedimentary processes not recorded below, such as sheet-floods and gravity flows. We include FA VI, FA VII and FA VIII in this association, because they often intercalate and show progressive passage between each other (Fig. 12).

The lower 200 m of the Río Correntoso Formation are dominated by coarse-grained sandstones deposited as sheet-floods (FA VI), interbedded with conglomerates (FA VII) showing sharp planar to erosive basal contacts. The uppermost 50 m of the Río Correntoso Formation are composed of an intercalation of sheet-floods (FA VI) and debris-flow deposits (FA VIII) in sharp planar contact. The passage of sandy, sheet-flood-dominated to conglomeratic debris flow-dominated deposits is interpreted as a progradation of an alluvial fan (Heward, 1977; Nielsen, 1982; Miall, 1985; Viseras and Fernández, 1994; Reading and Collinson, 1996; Suriano and Limarino, 2009). Additionally, this trend is also suggested by the thickening upward of the beds.

Temporal paleoenvironmental evolution

The measured section for the Miocene deposits south of Los Antiguos town is 980 meters thick and shows a general coarsening-upwards trend (Fig. 13) with transitional passage between the three Sedimentary units. The lowermost portion of the section is represented by the shallow marine deposits

of SU I (corresponding to the Centinela Formation) is up to 130 m thick. The base of this unit is covered, thus a thicker Miocene column than measured is expected if we consider the thickness lying in the subsurface. The boundary between these shallow marine deposits and the overlying fluvial deposits of SU II is gradual and not a sharp contact, as mentioned by Escosteguy *et al.* (2001), Dal Molin and Colombo (2003) for the study area. Similar relations were described (Cuitiño *et al.* 2012; 2015; 2019; Parras and Cuitiño, 2018) for nearby and other distant localities of the Austral-Magallanes Basin. In the study area, this transition consists of a stratigraphic interval that has particular sedimentological features with a thickness of about 50 m, which in this work is included into FA II, showing no evidences of a major temporal gap. Consequently the location of this boundary in the field is not straightforward. The passage from shallow and coastal marine deposits to the overlying fluvial environments suggests a regressive trend for the northern part of the Austral-Magallanes Basin during the early Miocene.

The sandstone/mudstone proportion along the measured column for fluvial deposits of SU II increases to the top. The higher proportion of mudstone deposits is recognized between 50 and 180 meters from the base of the column (Fig. 13). It includes the transitional marine deposits (Fig. 11) of the uppermost part of SU I as well as the lower segment of SU II; *i.e.* the upper part of the Centinela Formation and most of the Río Jeinemeni Formation. The lower terrestrial deposits represent a low sinuosity fluvial system with development of incipient paleosols on the floodplains (Fig. 11). This muddy interval shows a distinctive green-gray to dark-reddish coloration, which is visible and correlatable along several sites in the region, including strata of the Santa Cruz Formation (see Cuitiño *et al.*, 2019).

There is an upward decrease in the Accommodation/Sediment supply conditions (A/S ratio; Wright and Marriot, 1993; Shanley and McCabe, 1994; Catuneanu, 2006) marked by the passage from mudstone dominance and pedogenic features at the basal sector to channel-dominated with less floodplain deposits of SU II (*i.e.* Río Jeinemeni and Cerro Boleadoras formations). In parallel, the thickness of individual sandstone bodies progressively increases upward from 1.5 m up to 13 m. In turn, the upper part of SU II exhibits a large

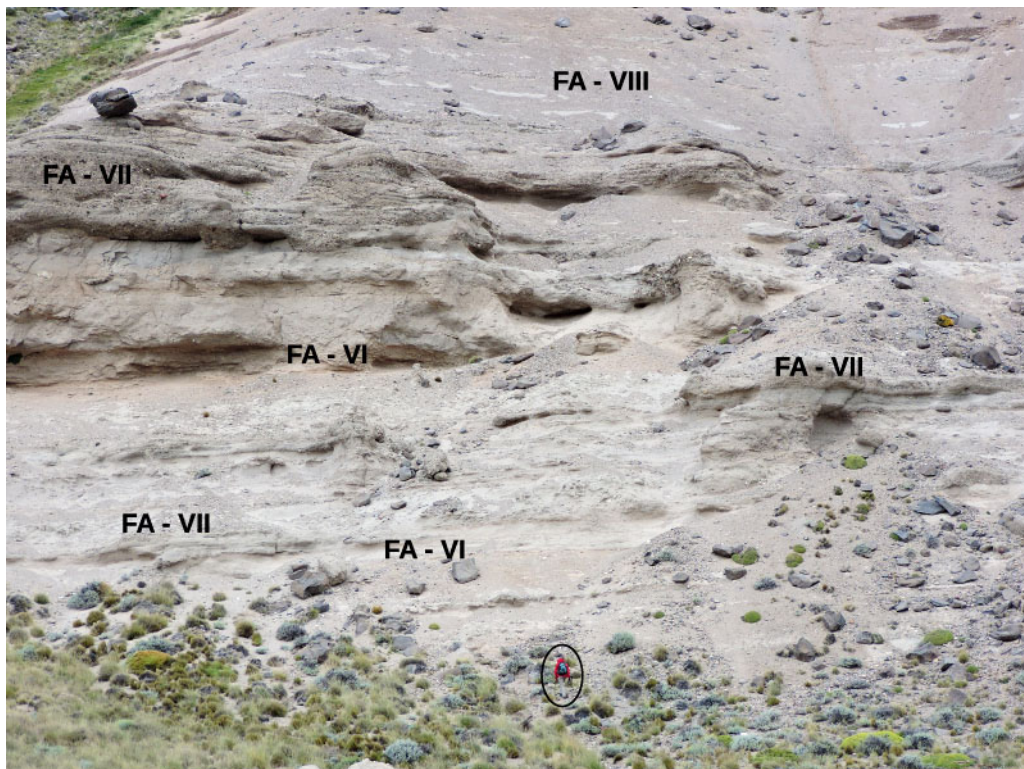


Figure 12. Outcrop overview of Sedimentary Unit III (SU III) (circle depicted a person scale of 1.6m high). Note the coarser deposits of this SU. Also the passage from one FA to another is also more chaotic compared with SU I and SU II.

variation in sandstone thickness reaching up to 15 m thick, with minor intercalated sandstone bodies of 2 to 5 m thick. The mid-portion of this interval displays a local increment of sandstones thickness reaching up 40 m, corresponding to the aeolian deposits of FA V. To the top of the fluvial deposits of FA II a slight grain-size increment is registered. Towards FA III, sandstone beds progressively diminish to the top from 12 m to 3 m thick.

It is noteworthy that in SU II some syn-sedimentary deformation structures are developed in the muddy Río Jeinemeni Formation, and at the lower sector of Cerro Boleadoras Formation, mostly affecting the fine-grained deposits of FA III and FA IV. This deformational evidence disrupts the original depositional arrangement and a complex imbrication of fault and folds is recognized (Lagabrielle *et al.*, 2010; Barberón *et al.*, 2018; Folguera *et al.*, 2018). This structure shows that deformation involves only a discrete stratigraphic interval, clearly bracketed by horizontal disposition of beds below and above (Fig. 14).

Conglomerates start to intercalate as lag deposits at the base of channels in the upper part of the fluvial system of SU II. From these first intercalations up to the top of the measured column,

the conglomerate/sandstone proportion can be used as a significant tectonostratigraphic indicator (Uba *et al.*, 2005; Suriano *et al.*, 2017). This proportion increases upwards and is especially recognized in the uppermost 150 meters, representing the alluvial fan deposits of SU III. This upper conglomeratic interval is distinctive of the study zone and not yet recognizable in other sites of the northern part of the Austral-Magallanes Basin. In parallel, conglomerate bodies display variations in thickness and internal arrangement. In the basal sector of SU III, fine-grained conglomerates progressively increase in thickness from 3 m to 7.5 m, showing clast-supported fabrics and massive to horizontal structures, being interspersed with coarse- to pebble-grained sandstones of FA VI. In the upper section of the SU III, conglomerate bodies reach up to 14 m thick and show matrix-supported fabrics and lack of tractive structures. Finally, SU III is covered in sharp contact with the basalts of Meseta Lago Buenos Aires Formation.

Upward shifting of sedimentary systems from marine to fluvial and finally to alluvial fan, suggests a progressively temporal loosening of accommodation space and increasing in slope. These processes can be related with the approaching of the orogenic

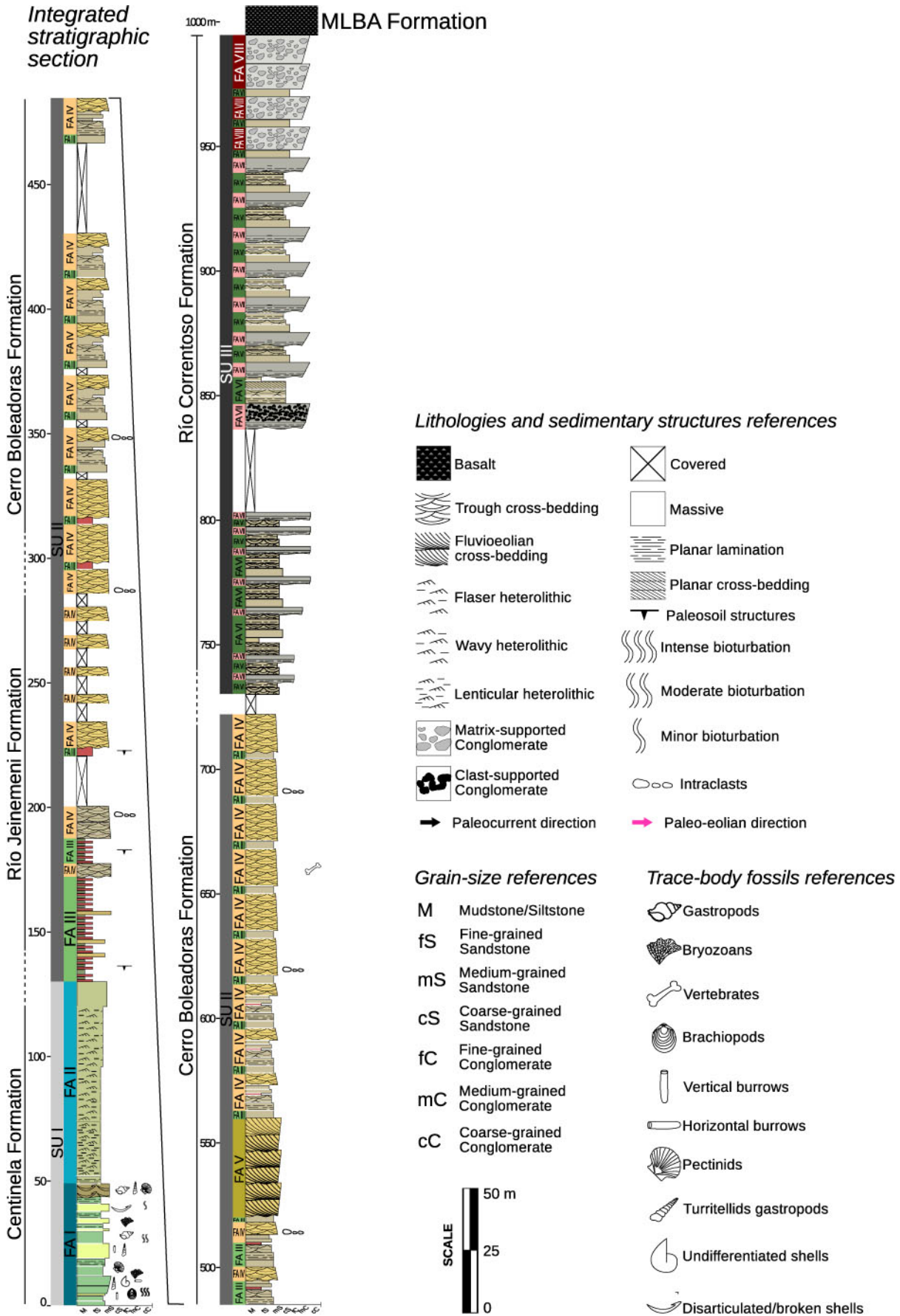


Figure 13. Vertical integrated stratigraphic section measured for the Miocene units south of Los Antiguos town (see location in Fig. 1).

front from west to east occurred during the Miocene (Thomson *et al.*, 2001; Ghiglione *et al.*, 2016b; 2018). This approximation is tangible within the facies associations, especially in the internal changing in SU II where incipient paleosols horizons are developed and then the fluvial channels dominates upwards.

Most of the available paleocurrent data from fluvial deposit of SU II (n = 12) indicates that transport of fluvial channels was towards the NE and E. Only locally fluvio-eolian interaction the paleo-eolian direction (n = 2) has a trend to the N-NE.

STRATIGRAPHIC AND TECTONIC IMPLICATIONS

The stratigraphic changes occurred in the Neogene deposits of the northern border of the Austral-Magallanes Basin can be related to coeval deformational processes in the adjacent Southern Patagonian Andes that affected the retroarc.

A sharp distinction can be made between the age-span of Oligocene-Neogene uplift processes affecting source areas from the mountains (either related to compression or isostatic rebound) and sedimentation in the Austral-Magallanes basin (Ghiglione *et al.*, 2016a). Thermochronological data clearly indicates exhumation related either to tectonics (faulting) and/or climatic (erosion-driven) processes between ~34 and 5 Ma that was accompanied by the onset of the Neogene sedimentation cycle. However, since top Miocene sediments of the study area yield a maximum age of 14 Ma (Blisniuk *et al.*, 2005) and are covered either by basalt lava flows or thin Quaternary conglomerates, there are not sequences representing significant volumes of rock younger than 14 Ma (Ghiglione *et al.*, 2016a; Cuitiño *et al.*, 2019). Therefore, from a geodynamic perspective, subsidence and sedimentation in the Austral-Magallanes Basin was coetaneous with the approach of the CSR, but the foreland depozone was abandoned at 14 Ma, *i.e.* during the subduction of several ridge's segments. It has been argued that collision produced a regional uplift of continental Patagonia (Guillaume *et al.*, 2013, Dávila *et al.*, 2018), and subsidence and sediments migrated towards the south in Austral-Magallanes Basin of Tierra del Fuego and Malvinas basins and eastward into the Argentine offshore basin (Ghiglione *et al.*, 2016a). The geodynamic setting during the middle Miocene included young and hot approaching oceanic crust from the CSR, *i.e.* positive buoyancy slab and shallower subduction

angle, indicating a possible episode of enhanced coupling between the South America and Nazca plates (Barberón *et al.*, 2018), with enhanced uplift and exhumation of the mountain domain, that ultimately generated a bypass surface in the Austral basin.

New chronological data from detrital zircons has recently shown that foreland basin sedimentation in the Austral basin has been relatively continuous throughout the Cenozoic (Fosdick *et al.*, 2015; Encinas *et al.*, 2018b). A pervasive regional unconformity at the base of the Oligocene sequences can be used to determine the base of sequences related to the first uplift pulses in response to the approach of the CSR, although synorogenic sedimentation started earlier, during the Eocene (Ligorio Marquez Formation in the northern depocenter; Encinas *et al.*, 2018b) or Eocene - Oligocene (Río Turbio and Río Guillermo formations in the south; Fosdick *et al.*, 2014). Our analysis is focused on the subsequent Miocene sequences. The presence of growth strata and syntectonic unconformities (Barberón *et al.*, 2018) implies that these deposits can be considered as syndeformational. We analyze the integrated stratigraphic section in a basin infill context trying to identify which basin model attached to these less explored outcrops in northwestern edge of the Austral-Magallanes Basin.

Microtectonic analysis, field data, digital elevation models (DEMs), satellite imagery and plate kinematic models are available for the areas surrounding the Lago Buenos Aires, which are the base for the understanding of the subduction dynamics of the Nazca Plate below the South American Plate. This subduction process is divided into two successive kinematic stages (Lagabrielle *et al.*, 2004, 2007; Scalabrino *et al.*, 2009, 2010): a pre-ridge subduction stage of "normal subduction", and a ridge subduction stage involving opening of slab windows, due to both slab tear and ridge axis subduction) (Scalabrino *et al.*, 2009). According to these deformational stages and the stratigraphic units deposited in the basin, two main steps in the development of clastic deposits could be identified: a regressive Late Eocene-Early Oligocene stage represented in the tectonically inverted Guadal Plateau (San José Formation, Flint *et al.*, 1994), which is followed by the studied Miocene sequences during the pre-ridge stage. Sedimentation stalled during the ridge collision stages.

Tectonostratigraphic stages

Our detailed stratigraphic and sedimentological analysis allows determining several tectonostratigraphic stages during pre-ridge subduction condition.

The first stage is represented by an important marine transgression, occurred during the early Miocene (22-18 Ma), in which a large part of southern Patagonia was flooded by the Atlantic sea (Feruglio, 1949; Malumián and Náñez, 2011; Encinas *et al.*, 2018a), including regions located in the foothills of the Southern Patagonian Andes (Cuitiño *et al.*, 2012; 2015). This stage could be related to the initial stages of the onset of a fold and thrust belt representing by the shallow marine deposition is typically recorded by the Centinela Formation and equivalents to the north and south of the study zone (Furque and Camacho, 1972; Chiesa and Camacho, 1995; Giacosa and Franchi, 1997; Cuitiño and Scasso, 2010; Parras *et al.*, 2012; Cuitiño *et al.*, 2015; 2019).

In a second step, continuous shortening and uplift of the Southern Patagonian Andes led to a shift from shallow marine to continental fluvial-alluvial conditions (Escosteguy *et al.*, 2003, Dal Molin and Colombo, 2003; Cuitiño *et al.*, 2019). These voluminous erosional products now form the Río Zeballos Group (Ugarte, 1956; Escosteguy *et al.*, 2003) and equivalent deposits of the Patagonian foothills. The transition from the Centinela Formation to the Río Zeballos Group marks the withdrawal of the Miocene Patagonian seaway. An approximately 1000 m thick sequence consisting of shallow marine to fluvial-alluvial sandstones, siltstones and conglomerates that record erosion of uplifted relief. However, there are multiple indications of syndepositional extensional faulting for the Jeinimeni Formation (Figs. 11 and 14; Dal Molin and Colombo, 2003), that could be related to plate uncoupling during the early Miocene plate reorganization (Barberón *et al.*, 2018).

A third stage is coeval with soft-sediment compressional deformation in the Río Jeinimeni Formation (Fig 14). Mudstones present in this unit are more sensitive to deformation during and immediately after sedimentation ceased. This deformational evidence could be related to seismic movements associated with the nearby Andean uplift (Barberón *et al.*, 2018) and/or due to a sedimentary structures internal collapse caused by sedimentary load. The main Cenozoic contractional tectonism

occurred during and after the deposition of the Río Zeballos Group and prior to the emplacement of 12 Ma basalts over an erosional surface that cross-cuts the last thrusts (Lagabrielle *et al.*, 2004; 2007; De La Cruz and Suárez, 2006; Guivel *et al.*, 2006).

Shallow marine deposits of SU I at the base of the integrated stratigraphic section could be related to a high accommodation space episode in the basin, linked with a subsided crustal setting (Scalabrino *et al.*, 2009, 2010; Lagabrielle *et al.*, 2004; 2007) probably related with an increment in orogenic load (Cuitiño *et al.*, 2015; Ghiglione *et al.*, 2016a; Dávila *et al.*, 2018). The passage from a shallow marine (SU I) to a continental fluvial environments (SU II) suggests the influence of allocyclic factors, which are principally supported by the losing of fine sediments deposits (floodplains and sheet-floods) upwards sequence (Walker and James, 1992; Reading and Collinson, 1996; Uba *et al.*, 2005). The passage from fluvial systems of SU II to alluvial fans of the SU III, the appearance of conglomeratic deposits at expense of sandstones bodies and amalgamation of channelized deposits is another evidence of a losing in accommodation space upwards sequence (Wright and Marriot, 1993, Suriano *et al.*, 2015; 2017).

Paleocurrents, measured in trough cross-bedded sandstones and pebble-sandstones from fluvial channel deposits, indicate that the sediment distribution was towards the NE-E. The internal coarsening upwards trend could be related to the progradation of these deposits linked with an active mountain uplift westwards, producing a NE sedimentary distribution pattern marking the influence of tectonic load in the western edge of Southern Patagonian Andes (Ghiglione *et al.*, 2016a). These distribution pattern is in concordance to the existing thermochronological data (Thomson *et al.*, 2001, 2010; Fosdick *et al.*, 2013; Guillaume *et al.*, 2013) that indicates enhanced exhumation that migrated eastward between ~33 Ma (from southern South America) and 5–3 Ma (Barberón *et al.*, 2018).

Meaning of the studied succession in the context of the Northern Austral-Magallanes Basin

The comparison between the surrounding areas with Miocene depositional sequences studied in this work, open the debate of the connectivity of the different sedimentary Miocene record areas (Folguera *et al.*, 2018; Encinas *et al.*, 2018b). The



Figure 14. Photographic panoramas looking to the NW of Río Jeinemeni exposures showing superposition of extensional and compressional deformational structures during deposition of the Río Jeinemeni Formation (lower Miocene) (modified from Barberón *et al.*, 2018). The red star represents an U-Pb age from Folguera *et al.*, 2018. Green and purple dots represent FA III and FA IV, respectively. These deposits are associated in Sedimentary Unit II, a mixed-load fluvial system. The subhorizontal, post-deformation strata belong to the Cerro Boleadoras Formation.

appearance of units of similar lithologies, and in some cases environmental interpretation, could lead the possibility of a connection between Guadal Plateau, Guenguel and the Northern Austral-Magallanes Basin. On the other hand, the structures and deformational patterns observed within these localities suggests that each depocenter underwent a particular deformational history. Possibly, the studied region was connected to other areas in pre-contractual stages. During the most important Andean uplift, and somewhat before basalts flows, these depocenters were probably disconnected.

The main concluding remark is that the Miocene beds of the northern Austral-Magallanes Basin could unravel the history of Andean uplift in the area. Taking into account *i)* the progradational environmental shift from shallow marine to continental alluvial fans depicted by three Sedimentary units; *ii)* the

deformational stages of pre- and post-collisional tectonic context; *iii)* the paleocurrents directions and *iv)* the soft sediment deformation in Río Jeinemeni Formation, the whole Neogene sedimentary section can be regarded as accumulated in a foreland basin system (DeCelles and Giles, 1996). The marine units at the foothills of the Southern Patagonian Andes are better explained by foreland basin subsidence due to flexural response to crustal thickening in the western Cordillera (Cuitiño *et al.*, 2012; 2015; Dávila *et al.*, 2018).

We acknowledge that additional work is needed to refine the accumulation model for the Miocene of the northern Austral-Magallanes Basin. Ongoing work on clay mineralogy and paleosol analysis will provide climatic constraints; which together to provenance analysis will be of great value to understand the evolution of this foreland basin system.

CONCLUSIONS

The study area is located in the retroarc of the Southern Patagonian Andes and records a foreland sedimentary basin infill, with a general coarsening-upwards trend indicating the progressive approximation of the deformational front. This sedimentary infill is divided into three Sedimentary Units related to marine-transitional to terrestrial paleoenvironments: *Sedimentary Unit I* represents a shallow marine, well-oxygenated and agitated environment, with some wave-influence in coastal marine beach environment; *Sedimentary Unit II* represents a mixed-load, low sinuosity fluvial system with an isolated episode of aridification; *Sedimentary Unit III* represents an alluvial fan with a passage from sandy, sheet-flood dominated to conglomeratic, debris flow-dominated deposits.

From these sedimentologic and stratigraphic analyses we conclude that the *Sedimentary Unit I* (Centinela Formation) is related to the initial stages of Andean uplift. The abrupt generation of accommodation space allowed the marine ingression from the Atlantic. *Sedimentary Unit II* (Río Jeinemeni and Cerro Boleadoras formations) depicted the *in situ* deformation during Andean uplift. These evidences are represented in the Río Jeinemeni cliff (Fig. 14) and the changing in accommodation space is marked by the increasing sandstone/mudstone ratio. Finally, *Sedimentary Unit III* (Río Correntoso Formation) is a clear evidence of this progressive and systematic loosing in accommodation space. The latter is the product of the eastward migration of the deformational front that finally produced the top bypass surface of the Neogene sequence.

Acknowledgements

This work has been carried out with the financial support of grant projects from Agencia Nacional de Promoción Científica y Técnica PICT 2013-0398 and PICT 2015-0792 to José Ignacio Cuitiño, and PICT-2013-1291 to Matías Ghiglione. Logistic facilities were supplied by CCT CONICET-CENPAT, IDEAN UBA-CONICET, and people from Estancia La Ascensión. We are grateful to people who helped during fieldwork and contributed during subsequent discussions: Rodrigo Suárez, Julieta Ventisky, Sergio Vizcaíno, Susana Bargo, Gonzalo Ronda, Miguel Ramos, Jonathan Toba. We are grateful to the

reviewers Andrés Folguera and César Viseras and the Invited Editor Augusto Varela, for their observations that considerably helped to improve the original version of this manuscript.

REFERENCES

- Aguirre Urreta, M.B., 1985.** Informe paleontológico de los perfiles de la cuesta del Oro, veranada de Gómez y boliche Mondelo, Cordillera Patagónica, provincia de Santa Cruz. Universidad Nacional de Buenos Aires, (inédito). Buenos Aires.
- Aguirre Urreta, M.B. and Ramos, V.A., 1981.** Estratigrafía y paleontología de la Alta Cuenca del río Roble, provincia de Santa Cruz. *Actas 8° Congreso Geológico Argentino*, 3:101-138. Buenos Aires.
- Aramendía, I., M.E. Ramos, S. Geuna, J.I. Cuitiño and M.C. Ghiglione, 2018.** A multidisciplinary study of the Lower Cretaceous marine to continental transition in the northern Austral-Magallanes basin and its geodynamic significance. *Journal of South American Earth Sciences*, 86:54-69.
- Barberón, V., G. Ronda, P.R. Leal, C. Sue and M.C. Ghiglione, 2015.** Lower Cretaceous provenance in the northern Austral basin of Patagonia from sedimentary petrography. *Journal of South American Earth Sciences*, 64:498-510.
- Barberón, V., C. Sue, M. Ghiglione, G. Ronda and E. Aragón, 2018.** Late Cenozoic brittle deformation in the Southern Patagonian Andes: Record of plate coupling/decoupling during variable subduction?. *Terra Nova*, 30(4):296-309.
- Blisniuk, P.M., L.A. Stern, C.P. Chamberlain, B. Idleman and P.K. Zeitler, 2005.** Climatic and ecologic changes during Miocene surface uplift in the Southern Patagonian Andes. *Earth and Planetary Science Letters*, 230(1-2):125-142.
- Boutonnet, E., N. Arnaud, C. Guivel, Y. Lagabrielle, B. Scalabrino and F. Espinoza, 2010.** Subduction of the South Chile active spreading ridge: A 17Ma to 3Ma magmatic record in central Patagonia (western edge of Meseta del Lago Buenos Aires, Argentina). *Journal of Volcanology and Geothermal Research*, 189(3):319-339.
- Bown, T.M. and C.N. Larriestra, 1990.** Sedimentary paleoenvironments of fossil platyrrhine localities, Miocene Pinturas Formation, Santa Cruz Province, Argentina. *Journal of Human Evolution*, 19:87-119.
- Bridge, J. S. and S.D. Mackey, 1993.** A revised alluvial stratigraphy model. In: *Alluvial sedimentation*. Special Publication International Association of Sedimentologists: 575.
- Bridge, J., and R. Demicco, 2008.** *Earth surface processes, landforms and sediment deposits*. Cambridge University Press: 835.
- Brookfield, M.E. and T.S. Ahlbrandt (Eds.), 2000.** *Eolian sediments and processes* (Vol. 38). Elsevier: 671.
- Busteros, A. and O. Lapido, 1983.** Rocas básicas en la vertiente noroccidental de la meseta del Lago Buenos Aires, provincia de Santa Cruz. *Revista Asociación Geológica Argentina*, 38(3-4):427-436.
- Catuneanu, O., 2006.** *Principles of sequence stratigraphy*. Elsevier (387).
- Chiesa, J.O. and H.H. Camacho, 1995.** *Litoestratigrafía del Paleógeno marino en el noroeste de la provincia de Santa Cruz, Argentina*. Monografías de la Academia Nacional de Ciencias Exactas, Físicas y Naturales de Buenos Aires, 11:9-15.
- Cuitiño, J.I. and R.A. Scasso, 2010.** Sedimentología y

- paleoambientes del Patagoniano y su transición a la Formación Santa Cruz al sur del Lago Argentino, Patagonia Austral. *Revista de la Asociación Geológica Argentina*, 66(3):406-417.
- Cuitiño, J.I., M.M. Pimentel, R. Ventura Santos and R.A. Scasso**, 2012. High resolution isotopic ages for the early Miocene "Patagoniense" transgression in Southwest Patagonia: Stratigraphic implications. *Journal of South American Earth Sciences*, 38:110-122.
- Cuitiño, J.I., R. Ventura Santos, P.J. Alonso Muruaga and R.A. Scasso**, 2015. Sr-stratigraphy and sedimentary evolution of early Miocene marine foreland deposits in the northern Austral (Magallanes) Basin, Argentina. *Andean Geology*, 42(3):364-385.
- Cuitiño, J.I., S.F. Vizcaíno, M.S. Bargo and I. Aramendía**, 2019. Sedimentology and fossil vertebrates of the Santa Cruz Formation (early Miocene) in Lago Posadas, southwestern Patagonia, Argentina. *Andean Geology*, 46:383-420.
- Dal Molin, C.N. and M. Franchi**, 1996. *Reinterpretación estratigráfica de las sedimentitas terciarias del sudoeste de Chubut*. In: XIII Congreso Geológico Argentino and III Congreso de Exploración de Hidrocarburos, Actas. Vol. 1, pp: 473-478.
- Dal Molin, C.N. and F. Colombo**, 2003. Sedimentación neógena en la Cuenca del Río Zeballos y del Río Jenimeni (47° de Latitud Sur). Antepaís Patagónico, Argentina. *Geogaceta* 34:139-142.
- Dávila, F.M., C. Lithgow-Bertelloni, F. Martina, P. Ávila, J. Nóbile, G. Collo and F. Sánchez**, 2018. *Mantle Influence on Andean and Pre-Andean Topography*. In: The Evolution of the Chilean-Argentinean Andes: 363-385. Springer, Cham.
- De Barrio, R.E., G. Schillato-Yané and M. Bond**, 1984. *La Formación Santa Cruz en el borde occidental del Macizo del Deseado (Provincia de Santa Cruz) y su contenido paleontológico*. 9° Congreso Geológico Argentino, Actas IV: 539-556.
- DeCelles, P.G. and W. Cavazza**, 1999. A comparison of fluvial megafans in the Cordilleran (Upper Cretaceous) and modern Himalayan foreland basin systems. *Geological Society of America Bulletin* 111:1315-1334.
- DeCelles, P.G. and K.A. Giles**, 1996. Foreland basin systems. *Basin research*, 8(2):105-123.
- De la Cruz, R. and M. Suárez**, 2006. *Geología del área Puerto Guadal-Puerto Sánchez, Región Aisén del General Carlos Ibáñez del Campo*. Servicio Nacional de Geología y Minería, Carta Geológica de Chile, Serie Geológica Básica 95: 58, 1 mapa escala 1:100.000. Santiago.
- De la Cruz, R; M. Suárez, M. Belmar, D. Quiroz and M. Bell**, 2003. *Área Coihaique-Balmaceda, Región de Aisén del General Carlos Ibáñez del Campo*. Servicio Nacional de Geología y Minería, Carta Geológica de Chile, Serie Geología Básica, 80: 40.
- Encinas, A., A. Folguera, F. Bechis, K.L. Finger, P. Zambrano, F. Pérez, P. Bernabé, F. Tapia, R. Riffo, L. Buatois, D. Orts, S.N. Nielsen, V. Valencia, J.I. Cuitiño, V. Oliveros, L.deG. Del Mauro and V.A. Ramos**, 2018a. The Late Oligocene–Early Miocene Marine Transgression of Patagonia. In: *The Evolution of the Chilean-Argentinean Andes*: 443-474. Springer, Cham.
- Encinas, A., A. Folguera, R. Riffo, P. Molina, L. Fernández Paz, V.D. Litvak and M. Carrasco**, 2018b. Cenozoic basin evolution of the Central Patagonian Andes: Evidence from geochronology, stratigraphy, and geochemistry. *Geoscience Frontiers*. <https://doi.org/10.1016/j.gsf.2018.07.004>
- Escosteguy, L., M. Franchi and C. Dal Molin**, 2001. *Formación Ligorio Márquez (Paleoceno superior-Eoceno inferior) en el río Zeballos, provincia de Santa Cruz, Argentina*. 11° Congreso Latinoamericano de Geología, 3° Congreso Uruguayo de Geología. Montevideo.
- Escosteguy, L., C. Dal Molín, M. Franchi, S. Geuna and O. Lapido**, 2003. *Hoja Geológica 4772-II Lago Buenos Aires*. Programa Nacional de Cartas Geológicas de la República Argentina 1:250.000. Servicio Geológico Minero, Boletín 339.
- Espinoza, F., D. Morata, E. Pelleter, R.C. Maury, M. Suárez, Y. Lagabrielle, M. Polvé, H. Bellon, J. Cotten, R. De La Cruz and C. Guivel**, 2005. Petrogenesis of the Eocene and Mio–Pliocene alkaline basaltic magmatism in Meseta Chile Chico, southern Patagonia, Chile: Evidence for the participation of two slab windows. *Lithos*, 82(3):315-343.
- Feruglio, E.**, 1949. *Descripción Geológica de la Patagonia*. Dirección General de Yacimientos Petrolíferos Fiscales, 3 Tomos, T1: 1-323; T2: 1-349; T3: 1-331. Buenos Aires.
- Flint, S.S., D.J. Prior, S.M. Agar and P. Turner**, 1994. Stratigraphic and structural evolution of the Tertiary Cosmelli Basin and its relationship to the Chile triple junction. *Journal of the Geological Society*, 151:251-268.
- Folguera, A., A. Encinas, A. Echaurren, G. Gianni, D. Orts, V. Valencia and G. Carrasco**, 2018. Constraints on the Neogene growth of the central Patagonian Andes at the latitude of the Chile triple junction (45–47° S) using U/Pb geochronology in synorogenic strata. *Tectonophysics*. <https://doi.org/10.1016/j.tecto.2018.06.011>
- Fosdick, J.C., M. Grove, J.K. Hourigan and M. Calderón**, 2013. Retroarc deformation and exhumation near the end of the Andes, southern Patagonia. *Earth and Planetary Science Letters*, 361:504-517.
- Fosdick, J. C., M. Grove, S.A. Graham, J.K. Hourigan, O. Lovera and B.W. Romans**, 2015. Detrital thermochronologic record of burial heating and sediment recycling in the Magallanes foreland basin, Patagonian Andes. *Basin Research*, 27(4):546-572.
- Furque, G.**, 1973. *Descripción geológica de la Hoja 58b, Lago Argentino, provincia de Santa Cruz*. Servicio Nacional Minero Geológico, Boletín 140:1-49.
- Furque, G. and H.H. Camacho**, 1972. *El Cretácico Superior y Terciario de la región austral del Lago Argentino, provincia de Santa Cruz*. Actas 4ª Jornadas Geológicas Argentinas, 3:61-75.
- Furque, G.**, 1973. *Descripción geológica de la Hoja 58b, Lago Argentino, provincia de Santa Cruz*. Servicio Nacional Minero Geológico, Boletín 140:1-49.
- García-Tortosa, F. J., P. Alfaro, L. Gibert and G. Scott**, 2011. Seismically induced slump on an extremely gentle slope (< 1) of the Pleistocene Tecopa paleolake (California). *Geology*, 39(11):1055-1058.
- Ghiglione, M. C., J. Quinteros, D. Yagupsky, P. Bonillo-Martínez, J. Hlebszevtich, V.A. Ramos, G. Vergani, D. Figueroa, S. Quesada and T. Zapata**, 2010. Structure and tectonic history of the foreland basins of southernmost South America. *Journal of South American Earth Sciences*, 29(2):262-277.
- Ghiglione, M.C., M. Naipauer, C. Sue, V. Barberón, V. Valencia, B. Aguirre-Urreta and V.A. Ramos**, 2015. U–Pb zircon ages from the northern Austral basin and their correlation with the Early Cretaceous exhumation and volcanism of Patagonia. *Cretaceous Research*, 55:116-128.
- Ghiglione M.C., C. Sue, M.E. Ramos, J.E. Tobal and R.E. Gallardo**, 2016a. The Relation Between Neogene Orogenic Growth in the Southern Andes and Sedimentation in the offshore

- Argentine and Malvinas basins during the Opening of the Drake Passage. In: *Geodynamic Evolution of the Southernmost Andes: Connections with the Scotia Arc*, p. 109-136. Springer International Publishing.
- Ghiglione, M., V.A. Ramos, J.I. Cuitiño and V. Barberón**, 2016b. Growth of the southern Patagonian andes (46–53° S) and their relation to subduction processes. In *Growth of the Southern Andes*: 201-240. Springer, Cham.
- Ghiglione M.C., G. Ronda, I. Aramendía, R. Suárez, M. Ramos, V. Barberón, J. Tobal E. Morabito, J. Martinod and C. Sue**, in press. Structure and tectonic evolution of the South Patagonian fold and thrust belt. In *Andean Tectonics*. Editors: Brian K. Horton and Andrés Folguera Ed. Elsevier.
- Giacosa, R. and M. Franchi**, 1997. *Hojas Geológicas 4772-III Lago Belgrano y 4772-IV Lago Posadas, escala 1:250.000, provincia de Santa Cruz*. Servicio Geológico Minero Argentino, 95 p., inédito.
- Giacosa, R. and M. Franchi**, 2001. *Descripción geológica de la Hoja 1:250.000, 4772-III y IV, Lago Posadas y Lago Belgrano, provincia de Santa Cruz, Argentina*. Buenos Aires, Boletín del Servicio Geológico Minero Argentino, 201:1-74.
- Gibling, M. R.**, 2006. Width and thickness of fluvial channel bodies and valley fills in the geological record: a literature compilation and classification. *Journal of Sedimentary Research*, 76(5):731-770.
- Gorring, M., S. Kay, P. Zeitler, V.A. Ramos, D. Rubiolo, M. Fernández and J. Panza**, 1997. Neogene Patagonian plateau lavas. Continental magmas associated with ridge collision at the Chile triple junction. *Tectonics*, 16(1):1-17.
- Guillaume, B., C. Gautheron, T. Simon-Labric, J. Martinod, M. Roddaz and E. Douville**, 2013. Dynamic topography control on Patagonian relief evolution as inferred from low temperature thermochronology. *Earth and Planetary Science Letters*, 364:157-167.
- Guivel, C., D. Morata, E. Pelleter, F. Espinoza, R.C. Maury, Y. Lagabrielle and M. Suárez**, 2006. Miocene to Late Quaternary Patagonian basalts (46–47° S): geochronometric and geochemical evidence for slab tearing due to active spreading ridge subduction. *Journal of Volcanology and Geothermal Research*, 149(3):346-370.
- Hatcher, J.B.**, 1897. Geology of Southern Patagonia. *American Journal Science*, 4, 4:327-354. New Haven.
- Hatcher, J. B.**, 1900. Sedimentary rocks of Southern Patagonia. *American Journal Science*, 9, 4:85-108. New Haven.
- Herries, R.D.**, 1993. Contrasting styles of fluvial–aeolian interactions at a downwind erg margin: Jurassic Kayenta–Navajo transition, northeastern Arizona, USA. In: *Characterization of Fluvial and Aeolian Reservoirs (Eds C.P. North and D.J. Prosser)*, Geological Society of London Special Publications, 73:199-218.
- Heward, A. P.**, 1977. Alluvial fan sequence and megasequence models: with examples from Westphalian D—Stephanian B coalfields, northern Spain: 669-702.
- Homocv, J.E.**, 1980. *Estudio estratigráfico de la comarca ubicada en el margen septentrional de la Meseta Belgrano, en la zona del Lago Posadas, Dpto. Río Chico, provincia de Santa Cruz*. Degree Thesis (Unpublished). Universidad de Buenos Aires, Departamento de Geología, Buenos Aires.
- Horton, B.K. and P.G. DeCelles**, 1997. The modern foreland basin system adjacent to the Central Andes. *Geology*, 25(10):895-898.
- Kidwell, S.M., Fürsich, F.T. and T. Aigner**, 1986. Conceptual framework for the analysis of fossil concentrations. *Palaios* 1:228-238.
- Kay, S. M., V.A. Ramos and M.L. Gorring**, 2002. *Geochemistry of Eocene Plateau Basalts related to ridge collision in Southern Patagonia*. XV Congreso Geológico Argentino (Calafate), Actas, Electronic files.
- Kidwell, S.M., Fürsich, F.T. and T. Aigner**, 1986. Conceptual framework for the analysis of fossil concentrations. *Palaios* 1:228-238.
- Kocurek, G. and K.G. Havholm**, 1993. Eolian sequence stratigraphy – a conceptual framework. In: *Recent Advances in and Applications of Siliciclastic Sequence Stratigraphy (Eds P. Weimer and H. Posamentier)*, AAPG Mem., 58:393-409.
- Kraemer P.E.**, 1998. Structure of the Patagonian Andes. Regional balanced cross section at 50° S.L. Argentina. *International Geology Review*, 40(10):896-915.
- Kraemer, P.E. and A. C. Riccardi**, 1997. Estratigrafía de la región comprendida entre los lagos Argentino y Viedma, Santa Cruz. *Revista de la Asociación Geológica Argentina*, 52 (3):333-360.
- Krapovickas, V.**, 2012. Deposits of the Santa Cruz Formation (late Early Miocene): paleohydrologic and paleoclimatic significance. *Early Miocene Paleobiology. In: Patagonia: High-Latitude Paleocommunities of the Santa Cruz Formation*: 91.
- Krauss, M. J.**, 1999. Paleosols in clastic sedimentary rocks: their geologic applications. *Earth-Science Reviews*, 47:41-70.
- Lagabrielle, Y., M. Suárez, E. A. Rossello, G. Hérial, J. Martinod, M. Régnier and R. De la Cruz**, 2004. Neogene to Quaternary evolution of the Patagonian Andes at the latitude of the Chile Triple Junction. *Tectonophysics*, 385:211-241.
- Lagabrielle, Y., M. Suárez, J. Malavielle, D. Morata, F. Espinoza, R. Maury, B. Scalabrino, L. Barbero, R. De La Cruz, E.A. Rossello and H. Bellon**, 2007. Pliocene extensional tectonics in Eastern Central Patagonian Cordillera: geochronological constraints and new field evidence. *Terra Nova*, 19:413-424.
- Lagabrielle, Y., B. Scalabrino, M. Suárez and J.F. Ritz**, 2010. Mio-Pliocene glaciations of Central Patagonia: New evidence and tectonic implications. *Andean Geology*, 37(2):276-299.
- Langford, R.P. and M.A. Chan**, 1989. Fluvial–aeolian interactions: Part II, ancient systems. *Sedimentology*, 36:1037-1051.
- Lapido, O.**, 1979. *Descripción geológica de la Hoja 51a, Los Antiguos, provincia de Santa Cruz*. Servicio Geológico Nacional, inédito.
- Malumán, N. and C. Nández**, 2011. The Late Cretaceous–Cenozoic transgressions in Patagonia and the Fuegian Andes: foraminifera, palaeoecology, and palaeogeography. *Biological Journal of the Linnean Society*, 103:269-288.
- Miall, A.D.**, 1977. A review of the braided-river depositional environment. *Earth-Science Reviews*, 13:1-67.
- Miall, A.D.**, 1985. Architectural-Element Analysis: A New Method of Facies Analysis Applied to Fluvial Deposits. *Earth-Science Reviews*, 22:261-308.
- Miall, A.D.**, 1988. Architectural elements and bounding surfaces in fluvial deposits: anatomy of the Kayenta Formation (Lower Jurassic), southwest Colorado. *Sedimentary Geology*, 55(3-4), 233-262.
- Miall, A.D.**, 2006. *The Geology of Fluvial Deposits: Sedimentary facies, basin analysis, and petroleum geology, 4th Edition*. Berlin: Springer.
- Mjøs, R., Walderhaug, O. and Prestholm, E.**, 1993. Crevasse splays sandstone geometries in the Middle Jurassic Ravenscar Group Yorkshire, UK. In: Marzo, M., Puigdefábregas, C. (Eds.). Alluvial Sedimentation. *International Association of*

Sedimentologists Special Publication 17:167-184.

- Nilsen, T. H.**, 1982. Alluvial fan deposits. In: Scholle, P.A. and Spearing, D. (Eds.). *Sandstone Depositional Environments. American Association of Petroleum Geologists Memoir* 31:49-86.
- North, C.P. and S.K. Davidson**, 2012. Unconfined alluvial flow processes: recognition and interpretation of their deposits, and the significance for palaeogeographic reconstructions. *Earth-Science Reviews* 111, 199-223.
- Overeem, I.**, 2004. Rivers and floodplains: forms, processes, and sedimentary record. In: BRIDGE, J.S. (Ed). Blackwell Science, Oxford. *Journal of Quaternary Science* (491).
- Parras, A.M., and J.I. Cuitiño**, 2018. The stratigraphic and paleoenvironmental significance of the regressive Monte Observación Member, early Miocene of the Austral-Magallanes Basin, Patagonia. *Latin American Journal of Sedimentology and Basin Analysis*, 25:93-115.
- Parras, A., G.R. Dix and M. Griffin**, 2012. Sr-isotope chronostratigraphy of Paleogene-Neogene marine deposits: Austral Basin, southern Patagonia (Argentina). *Journal of South American Earth Sciences*, 37:122-135.
- Perkins, M.E., F.G. Fleagle, M.T. Heizler, B. Nash, T.M. Bown, A.A. Tauber and M.T. Dozo**, 2012. Tephrochronology of the Miocene Santa Cruz and Pinturas Formations, Argentina. In *Early Miocene Paleobiology in Patagonia: high-latitude paleocommunities of the Santa Cruz Formation (Vizcaino, S.F.; Kay, R.F.; Bargo, M.S.; editors)*. Cambridge University Press: 23-40. Cambridge.
- Pankhurst, R., T. Riley, C. Fanning and S. Kelley**, 2000. Episodic Silicic Volcanism in Patagonia and the Antarctic Peninsula: Chronology of magmatism associated with the Break-up of Gondwana. *Journal of Petrology*, 41:605-625.
- Quiroz, D. and Z. Bruce**, 2010. *Geología del Área Puerto Ingeniero Ibáñez-Villa Cerro Castillo, Región Aisén del General Carlos Ibáñez del Campo*. Servicio Nacional de Geología y Minería, Carta Geológica de Chile, Serie Geología Básica 124: 48, 1 mapa escala 1:100.000.
- Ramos, V.A. and S.M. Kay**, 1992. Southern Patagonian plateau basalts and deformation: backarc testimony of ridge collisions. *Tectonophysics*, 205(1-3):261-282.
- Ramos, V.A.**, 1979. *Tectónica de la región del río y lago Belgrano, Cordillera Patagónica, Argentina*. Actas II Congreso Geológico Chileno, 1:1B-32.
- Ramos, V.A.**, 1989. Andean foothills structures in northern Magallanes Basin, Argentina. *AAPG Bulletin*, 73(7):887-903.
- Reading, H.G. and J.D. Collinson**, 1996. Clastic coasts. En H.G. Reading (Ed.), *Sedimentary Environments: processes, facies and stratigraphy*, 3rd. Blackwell Science, Oxford: 232-280.
- Reineck, H. and F. Wunderlich**, 1968. Classification and origin of flaser and lenticular bedding. *Sedimentology*, 11: 99-104.
- Retallack, G.J.**, 2001. *Soils of the past: an introduction to paleopedology*. John Wiley and Sons: 407.
- Richiano, S.M., A.N. Varela, A., Cereceda and D.G. Poiré**, 2012. Evolución paleoambiental de la Formación Río Mayer, Cretácico Inferior, Cuenca Austral, Patagonia Argentina. *Latin American Journal of Sedimentology and Basin Analysis* 19: 3-26.
- Richiano, S., A.N. Varela, L. Gómez-Peral, A. Cereceda and D.G. Poiré**, 2015. Composition of the Lower Cretaceous source rock from the Austral Basin (Río Mayer Formation, Patagonia, Argentina): Regional implication for unconventional reservoirs in the Southern Andes. *Marine and Petroleum Geology* 66:764-790.
- Richiano, S., A.N. Varela and D.G. Poiré**, 2016. Heterogeneous distribution of trace fossils across initial transgressive deposits in rift basins: an example from the Springhill Formation, Argentina. *Lethaia* 49:524-539.
- Rivas, H., E. Bostelmann, J. Le Roux and R. Ugalde**, 2015. *Fluvial facies and architecture of the late middle Miocene, Mayoan, deposits of Chilean Patagonia*. In: XIV Congreso Geológico Chileno, Actas, Vol. 1:812-815.
- Salze, M., J. Martinod, B. Guillaume, J.J. Kermarrec, M. Ghiglione and C. Sue**, 2018. Trench-parallel spreading ridge subduction and its consequences for the geological evolution of the overriding plate: Insights from analogue models and comparison with the Neogene subduction beneath Patagonia. *Tectonophysics*, 737:27-39.
- Scalabrino B, Y. Lagabrielle, A. de la Rupelle, J. Malavieille, M. Polvé, F. Espinoza, D. Morata and M. Suárez**, 2009. Subduction of an active spreading ridge beneath southern South America: a review of the Cenozoic geological records from the Andean foreland, central Patagonia (46–47° S). *Subduction Zone Geodynamics*. Springer, Berlin: 227–246.
- Scalabrino, B., Y. Lagabrielle, J. Malavieille, S. Dominguez, D. Melnick, F. Espinoza and E.A. Rossello**, 2010. A morphotectonic analysis of central Patagonian Cordillera: Negative inversion of the Andean belt over a buried spreading center? *Tectonics*, 29(2).
- Schumm, S. A.**, 1981. Evolution and response of the fluvial system, sedimentologic implications. *Society of Economic Paleontologists and Mineralogists (SEPM) Special Publication*, 31:19-29.
- Shanley, K. W. and P. J. McCabe, P. J.**, 1994. Perspectives on the sequence stratigraphy of continental strata. *AAPG bulletin*, 78(4):544-568.
- Sinito, A. M.**, 1980. Edades geológicas, radimétricas y magnéticas de algunas vulcanitas cenozoicas de las provincias de Santa Cruz y Chubut. *Revista Asociación Geológica Argentina*, 35: 332-339.
- Sohn, Y. K., C. W. Rhee and B.C. Kim**, 1999. Debris flow and hyperconcentrated flood-flow deposits in an alluvial fan, northwestern part of the Cretaceous Yongdong Basin, Central Korea. *The Journal of Geology*, 107(1):111-132.
- Sruoga, P., M.S. Japas, F.M. Salani and L.E. Kleiman**, 2014. La Peligrosa caldera (47° 15' S, 71° 40' W): a key event during the Jurassic ignimbrite flare-up in Southern Patagonia, Argentina. *Journal of Volcanology and Geothermal Research*, 269:44-56.
- Suárez, M.**, 1976. Plate-tectonic model for southern Antarctic Peninsula and its relation to southern Andes. *Geology*, 4(4): 211-214.
- Suárez, M., R. De la Cruz and A. Troncoso**, 2000. Tropical/subtropical upper Paleocene–lower Eocene fluvial deposits in eastern central Patagonia, Chile (46° 45' S). *Journal of South American Earth Sciences*, 13(6):527-536.
- Suárez, M.**, 1976. Plate-tectonic model for southern Antarctic Peninsula and its relation to southern Andes. *Geology*, 4(4): 211-214.
- Suriano, J., and C.O. Limarino**, 2009. Sedimentación pedemontana en las nacientes del Río Jáchal y Pampa de Gualilán, Precordillera de San Juan. *Revista de la Asociación Geológica Argentina*, 65(3):516-532.
- Suriano, J., C. O. Limarino, A. M. Tedesco and M.S. Alonso**, 2015. Sedimentation model of piggyback basins: Cenozoic examples of San Juan Precordillera, Argentina. *Geological*

- Society, London, Special Publications*, 399(1):221-244.
- Suriano, J., D. Mardonez, J.B. Mahoney, J.F. Mescua, L.B. Giambiagi, D. Kimbrough and A. Lossada**, 2017. Uplift sequence of the Andes at 30 S: Insights from sedimentology and U/Pb dating of synorogenic deposits. *Journal of South American Earth Sciences*, 75:11-34.
- Taylor, A.M. and R. Goldring**, 1993. Description and analysis of bioturbation and ichnofabric. *Journal of Geological Society*, 150: 141-148. London.
- Thomson S.N., F. Hervé and B. Stockhert**, 2001. The Mesozoic-Cenozoic denudation history of the Patagonian Andes (southern Chile) and its correlation to different subduction processes. *Tectonics*, 20:693-711.
- Thomson S.N., M.T. Brandon, P.W. Reiners, J.H. Tomkin, C. Vásquez and N.J. Wilson**, 2010. Glaciation as a destructive and constructive control on mountain building. *Nature*, 467 (7313), 313.
- Ton-That, T., B. Singer, N.A. Mörner and J. Rabassa**, 1999. Datación de lavas basálticas por $^{40}\text{Ar}/^{39}\text{Ar}$ y geología glacial de la región del Lago Buenos Aires, Provincia de Santa Cruz, Argentina. *Revista de la Asociación Geológica Argentina*, 54(4):333-352.
- Uba, C. E., C. Heubeck and C. Hulka**, 2005. Facies analysis and basin architecture of the Neogene Subandean synorogenic wedge, southern Bolivia. *Sedimentary Geology*, 180(3-4):91-123.
- Ugarte, F.R.E.**, 1956. El grupo Río Zeballos en el flanco occidental de la Meseta Buenos Aires (Provincia de Santa Cruz). *Revista de la Asociación Geológica Argentina*, 11 (3):202-216.
- Van Loon, A. J.**, 2009. Soft-sediment deformation structures in siliciclastic sediments: an overview. *Geologos*. 15 (1):3-55.
- Varela, A.N., D.G. Veiga and D.G. Poiré**, 2012. Sequence stratigraphic analysis of Cenomanian greenhouse palaeosols: a case study from southern Patagonia, Argentina. *Sedimentary Geology*, 271-272:67-82.
- Varela, A.N., L.E. Gómez-Peral, S. Richiano and D.G. Poiré**, 2013. Distinguishing similar volcanic source areas from an integrated provenance analysis: implications for foreland Andean basins. *Journal of Sedimentary Research*, 83(3):258-276.
- Veiga, G.D., L.A. Spalletti and S. Flint**, 2002. Aeolian/fluvial interactions and high-resolution sequence stratigraphy of a non-marine lowstand wedge: the Avilé Member of the Agrio Formation (Lower Cretaceous), central Neuquén Basin, Argentina. *Sedimentology*, 49(5):1001-1019.
- Viseras, C. and Fernández, J.**, 1994. Channel migration patterns and related sequences in some alluvial fan systems. *Sedimentary Geology*, 88: 201-217.
- Viseras, C., S. Henares, L.M. Yeste and F. García-García**, 2018. Reconstructing the architecture of ancient meander belts by compiling outcrop and subsurface data: A Triassic example. In: Meandering Rivers. *International Association of Sedimentologists, Special Publications*, 48:419-444.
- Walker, R.G. and N. James**, 1992. *Facies, facies model and modern stratigraphic concepts*. Facies model: response to sea level change. Geological Association of Canada: 407.
- Wasson, R.J.**, 1974. Intersection point deposition on alluvial fans: an Australian example. *Geografiska Annaler. Series A. Physical Geography*: 83-92.
- Wright, V.P. and S. B. Marriott**, 1993. The sequence stratigraphy of fluvial depositional systems: the role of floodplain sediment storage. *Sedimentary Geology*, 86(3-4):203-210.
- Zapata, L., V. Krapovickas, M. S. Raigemborn and S. D. Matheos**, 2016. Bee cell trace fossils associations on paleosols from the Santa Cruz Formation: Palaeoenvironmental and palaeobiological implications. *Palaeogeography, palaeoclimatology, palaeoecology*, 459:153-169.
- Zerfass, H., V.A. Ramos, M.C. Ghiglione, M. Naipauer, H.J. Belotti and I.O. Carmo**, 2017. Folding, thrusting and development of push-up structures during the Miocene tectonic inversion of the Austral Basin, Southern Patagonian Andes (50° S). *Tectonophysics*, 699:102-120.